GEOMETRICAL EFFECTS IN THE CONDUCTIVITY OF LOW DIMENSIONAL STRUCTURES.

BY

SYLVESTER A. HATWAAMBO

A DISSERTATION SUBMITTED TO THE UNIVERSITY OF ZAMBIA IN PARTIAL FULFILMENT OF THE REQUIREMENTS FOR THE AWARD OF THE DEGREE OF MASTER OF SCIENCE IN PHYSICS.

THE UNIVERSITY OF ZAMBIA

LUSAKA

1994

DECLARATION

I solemnly declare that this dissertation represents my own work which has not been submitted for a degree at this or any other University.

Signature .....

DEDICATION

I dedicate this work to my father, Edward Hatwaambo, my wife and to my children.

This dissertation of Sylvester Albert Hamusonde Hatwaambo is approved as fulfilling part of the requirements for the award of the Master of Science Degree in Physics by the University of Zambia.

Supervisor's signature .....

Date ..... Feb 4, 1994 .....

Co-supervisor's signature .....

Date .....

ABSTRACT

This work is an experimental study on percolation and electrical conductivity in two-dimensions with an aim of confirming some of the theoretical predictions, and measuring some of the parameters introduced in the theory. These parameters include the percolation threshold p_c , the critical exponents β and t for the percolation probability P(p) and electrical conductivity σ respectively. We wish to compare the electrical conductivity versus the probability of removed sites (1-p) for the four different common lattice types namely square, triangular, kagome' and honeycomb lattices. In particular, we wish to determine the percolation threshold p_c for these lattices experimentally and obtain the electrical conductivity critical exponent t within the critical regions of these geometrical lattices. We further wish to show the dependence of the system size length L on the electrical conductivity for the four different lattices mentioned above and obtain the value of t/ν, where ν is the correlation length critical exponent.

PREFACE

The following is a brief description of the individual chapters of this dissertation. In chapter one, we give definitions of terms used in the text and we also give a brief background to the percolation problem and conductivity. In chapter two, we give a brief description of the experimental techniques used. In chapter three, we present and analyse our results. In chapter four, we conclude our findings pertaining to the four geometrical lattices. Finally, in the appendix **A4** we give a detailed derivation of the electrical conductivity of a thin film without using the Boltzmann equation. This work became apparent when we were looking at the transport properties in thin films as part of the Graduate courses in Solid State Physics. May I take this opportunity to sincerely thank Dr. David Thompson for his assistance in this derivation.

ACKNOWLEDGEMENTS

My sincere thanks go to Prof. C.V. Sheth, supervisor of my work at the University of Zambia, and to Dr. D. Thompson, co-supervisor of my work who has since left the University of Zambia for the Universitie De Catolica, Peru, in South America. Both of these suggested the topic of my dissertation. I wish to thank the Birmingham University, School of Physics and Research, under the link programme for technical and material assistance rendered to me. I wish to extend my sincere thanks to the Head, Physics Department and the entire Physics Department staff for their assistance and co-operation that I dearly needed. I wish to thank all the technicians especially those from the Solid State Laboratory for their continued help.

Lastly but not the least, I wish to thank the Directorate of Human Resource Development and Training for sponsoring my studies at the University of Zambia.

CONTENTS page

CHAPTER ONE. INTRODUCTION

1.1 PREVIEW AND DEFINITIONS

Many systems show a change of phase or a change of symmetry under suitable conditions. This change of phase is called a phase transition. When iron is cooled below a critical temperature of about 1043K [1] in zero magnetic field for example, a spontaneous magnatization sets in and the system becomes ferromagnetic. Above this critical temperature, the spontaneous magnatization vanishes and the system becomes a paramagnet. However, within the critical temperature region (critical region), there is a spontaneous broken symmetry and the spontaneous magnetization follows a simple power law dependence [2]. It is the critical phenomena exhibited within the critical region in percolation theory that relate it to the thermal dynamic phase transitions.

There are very few phase transitions for which exact theoretical solutions are available and one of these is the percolation problem [3,4,5,6,7] in two dimensions. Although percolation has many definitions, we may define percolation as a slow movement of a liquid through a

porous material. This definition can be generalised to include such phenomena as conductivity, magnetism, specific heat, communication and all those systems that show phase transitions. The excitement in the percolation model lies in its almost game-like mathematical aspects. The fact that percolation model provides a well defined, transparent and intuitively satisfying model for spatially random processes, makes it easier to comprehend. Percolation in a static medium deals with a collection of points in space. These points may be adjacent or linked or connected in a random fashion depending on whether one is looking at bond-percolation or site-percolation. If the points have fixed positions and random linkages are made between them, then the system is a bond-type percolation. However, if the points are random and the linkages are determined by a rule which depends on the positions, then the system is a site-type percolation. There are also situations whereby both site and bond percolation may be used [3]. A system is said to be random if any chosen bond or site is independent of the state of the neighbouring bonds or sites.

A path is said to exist between two points of the distribution if a sequence of points can be found such that

successive points in a sequence are adjacent. The first adjacent points are known as the first nearest-neighbours and the second adjacent points are the second nearest-neighbours etc. There may be many paths between a given pair of points but if there is at least one path, then the points are said to be connected or linked. In many applications, it is of interest to know the probability that a given pair of points is connected or linked. A point will be connected or linked with a probability (p) and unconnected with a probability (1-p). The presence of a path may for example, allow the flow of fluid or charge between the points it connects, it may allow the spread of disease from one point to another or the passage of a telephone message from one point to the other etc.

The points of the distribution may be partitioned into clusters such that pairs of points in the same cluster are connected but there is no path between points in different clusters. The cluster sizes increase with the number of linkages and this cluster size variation as a function of the system parameters is of interest in percolation. A percolating state is reached when the cluster size extends to the boundaries of the system. The probability that a given point belongs to an infinite

cluster or percolating cluster, is known as the percolation probability P(p). In the flow of charge context, percolation probability will be the probability that charge introduced at a point will percolate or flow away indefinitely. This transition from a non-percolating state to a percolating state or vice-versa, is a kind of phase transition whereby the system changes from one state to another. Clearly, there must exist a critical point where the system turns from percolating to non-percolating. It is this critical regime about the critical point which has concerned most physicists. Percolation transition is purely a geometrical phenomena in which clusters are clearly defined static objects, which can grow to infinity by addition of a cluster or clusters at random.

1.2 Application of percolation.

The practical importance of percolation theory resides in its applicability to a broad range of physical phenomena. Its relevance to experimentalists is that it can be used to predict values of the percolation threshold p_c and the behaviour of physical properties within the critical region. As a rule, the value of the percolation threshold is structure dependent, namely that it is sensitive to short-range correlations in the system i.e the type of lattice, the interactions between materials in a continuum etc. For example, Zallen [8] and Shante and Kirkpatrick [4] give the values of the percolation threshold for both site and bond percolation. For site percolation [8], square lattice has a $p_c = 0.59$, triangular lattice has $p_c = 0.50$, kagome' lattice has $p_c = 0.65$ and honeycomb lattice has $p_c = 0.70$.

On the other hand, it is believed that the critical behaviour of such properties as the conductivity, specific heat, magnetization, elasticity, superconductivity, correlation length etc, are universal i.e, they do not depend on the existence of the lattice or local structure, even on the short-range interactions. This belief is based

upon the observation that, near p_c the correlation length is very much larger than the elementary length scale (lattice parameter), so that the local structure and interactions have no influence on cluster size and shape, and therefore on physical properties of the system.

A few of the cited examples on phase transition [4,8,9,10] are as follows; the flow of liquid in a porous medium is a kind of percolation in which the transition is from local wetting to extended wetting. The spread of disease in a population or orchard is a type of transition from containment to an epidemic. Communication or resistor network is a transition from disconnected to connected. Percolation in a conductor-insulator composite materials is a transition from insulator to metal. In composite superconductor-metal materials, the transition is from metal to superconducting whilst in thin helium films on surfaces, the transition is from normal to superfluid. Dilute magnets can exhibit a transition from paramagnetic to ferromagnetic and in glass transition, the system changes from liquid to glass etc.

1.3 Critical exponents and finite size scaling

Current phase transition theory suggests that the behaviour of the various systems mentioned in section 1.2, is likely to be described by a few universal parameters in the neighbourhood of the critical probability. These universal parameters are known as the critical exponents.

Near the critical point, there exists different phases which could be related to the co-existence of fluctuations on all length scales. Hence a theory that describes a system near the critical point must take account the entire spectrum of length scales. Due to multiple scale lengths, theoretical explanation of such systems become very complicated. However, Renormalisation Group Theory introduced in 1971 by K.G.Wilson [11] seems to give some light to the problem dealing with multiple scale lengths. In particular, the critical behaviour of fluids, ferromagnets, liquid mixtures and alloys could all be described by a single theory. Applications of real space renormalisation (also known as position-space renormalisation) to percolation is more or less equivalent to finite size scaling as we are dealing with position space situation. A relation that connects any two or more

critical exponents is known as the scaling relation. The critical exponent t for electrical conductivity in the percolation problem could be related to the static critical exponents β and ν for percolation probability and correlation length respectively, through the Alexander and Orbach [12] rule given in equation (1.4.4). The probability that an arbitrary selected site belongs to the largest cluster of a system behaves in the following fashion depending on the size of the system. For an infinitely large system, the largest cluster is infinitely large above the percolation threshold. And if its size is divided by the system size Length L, the ratio is finite i.e, $P(p) >> 0$ for $p > p_c$. For the concentration p below p_c, even the largest cluster is relatively small and the ratio of its size to the lattice size goes to zero, i.e, $P(p) = 0$ for $p < p_c$. Within the critical region, percolation probability P(p) follows a simple power law as

$$P(p) \sim |p-p_c|^{\beta} . \qquad (1.3.1)$$

The value of the critical exponent β is very difficult to determine precisely and current estimates of β range

between 0.4 and 0.5 [4] depending on the method used. For example, Kirkpatrick [13] showed that β was in the range between 0.3 and 0.4 in 3-dimensions. Gawlinski and Stanley [14], found the value of β to be 0.14 ± 0.02 in 2-dimensions. They further argued that the value of β depends on the value of the percolation threshold p_c. Zallen [8], quotes the value of β as equal to 0.14. In the case of a finite system, percolation probability depends not only on the concentration p but also on the linear dimension of the system L. In the asymptotic limit, $1/L \to 0$ for large lattices and $|p-p_c| \to 0$ close to threshold, and from finite size scaling [3], we expect percolation probability to follow

$$P(p) = L^{-\beta/\nu} F[(p-p_c)L^{1/\nu}], \qquad (1.3.2)$$

where F is some scaling function and ν the correlation length exponent. Through scaling arguments, we can write the correlation length from equation (1.3.2) as

$$\xi(p) \sim |p-p_c|^{-\nu} \qquad (1.3.3)$$

of the system. If this correlation length is much smaller

than the system size length L, i.e if

$$|p-p_c| >> L^{-1/\nu}, \qquad (1.3.4)$$

then we do not see the boundaries of the system and quantities averaged over the whole volume behave as an infinitely large system. In other words, for a very large system the size of the correlation length is negligible compared to the system size. If the correlation length is of the order of the system size length, then equation (1.3.3) becomes

$$L(p) \sim |p-p_c|^{-\nu}. \qquad (1.3.5)$$

1.4 Percolation and conductivity

For a square cubic shape of length L, the conductivity σ is equal to L^{2-d} multiplied by the current produced by unit voltage [3], where d is the dimensionality of the lattice. Here we set the distance between neighbouring points on the lattice equal to unity. It is obvious that, for large lattices we have zero conductivity if no infinite network of neighbours is

present i.e for $p < p_c$, then $\sigma = 0$. If however $p >> p_c$, then we have an infinite network and conductivity as well as probability of sites in the infinite network increase roughly linearly with the concentration p. As the concentration p equals unity, percolation probability also reaches unity and the conductivity reaches the bulk value. Since there seems to be close relationship between conductivity and percolation probability, Ziman [15] argued that the mobility of an electron in a disordered semiconductor should be given by a solution of the classical percolation problem. Similarly, Eggarter and Cohen [16] assumed that the mobility of an electron should be proportional to the percolation probability. It was not until 1971, when Last and Thouless [17], with their table-top experiment, measured the conductivity of sheets of conducting graphite paper with randomly punched holes distributed on a square lattice, that the above assumptions were disproven. Their results showed that electrical conductivity and percolation probability were not proportional. The reason being that dead ends do not contribute to the electrical current they carry but contribute to the mass or backbone of the infinite

network. Thus, most of the mass contained in percolation probability make no contribution to the electrical conductivity and therefore the critical exponent for electrical conductivity differs from that of percolation probability,(c.f. sect. 1.3 and 1.4). Last and Thouless however, did not attempt to estimate the values of the critical exponents for either electrical conductivity or percolation probability. As mentioned above, there is a very important region very close to the percolation threshold (the critical region) in which $|p-p_c| << 1$. In this regime, the percolation functions are observed to obey power law dependences on the distances from threshold $|p-p_c|$. One common and easy percolation function is the electrical conductivity whose power law dependence is as follows;

$$\sigma \sim |p-p_c|^t. \qquad (1.4.1)$$

The value of the critical exponent t has been evaluated both mechanically and by computer simulations [5].

The modern history of percolation as a physically observable critical phenomenon starts really with the experiment of Watson and Leath [18], who were the first to show that near p_c, the above relationship in

equation (1.4.1) holds. They measured the electrical conductivity of a 137 x 137-site simple square screen mesh versus the concentration of removed sites and reported the value of the critical exponent t as 1.34 ± 0.12 with the value of the percolation threshold $p_c = 0.413 \pm 0.005$ in two dimensions. Zallen [8] quotes the experimentally observed value of t in two dimensions as equal to 1.1 within the critical region $|p-p_c| \sim 0.1$.

Kirkpatrick [13], on his resistor network models showed that the value of the critical exponent ranged as follows; $1.5 \leq t \leq 1.6$ in two dimensions. Fogelholm [19], in his calculation of the electrical conductivity of a large finite random lattice, found the value of the exponent $t = 1.31 \pm 0.04$. This was apparently bond percolation on a square lattice and the critical region range was $0.005 < \varepsilon < 0.08$ where $\varepsilon = |p-p_c|$. Smith and Lobb [20] in their two dimensional conductor-insulator network measured the electrical conductivity exponent as t = 1.30, at a percolation threshold $p_c = 0.41$. Han K.H, Lim Z.S, and Lee Sung-Ik [21] on their random two dimensional swiss cheese percolating system, found the value of $t = 1.29 \pm 0.06$

with $p_c = 0.312 \pm 0.008$. These studies show that as the critical probability is approached, the paths through the system get more and more contorted and restricted. This is of course much easier to see in two dimensions than in three dimensions, since in two dimensions, a single picture can be used to display the whole system.

It should be emphasized that p_c varies greatly from lattice to lattice. However, the remarkable feature of the power law dependencies is that, the exponents do not depend on the details of the lattice geometry, but are the same for all lattices of the same Euclidian dimensionality. These exponents are also known as dimensional invariants. Each exponent has a fixed value for a given dimensionality without the specific nature of the short range structure. It should be noted also that for the same dimensionality, critical exponents are observed to be the same for both site and bond processes.

Since the bulk electrical conductivity of an infinite sample varies as $(p-p_c)^t$ near p_c (c.f. equation (1.4.1)), it can be argued that the average conductivity $\langle\sigma\rangle$ of a finite sample at p equal to p_c is given by [22] as

$$\langle\sigma\rangle = L^{-t/\nu}[c_1 + c_2 f_2(L) + ...], \qquad (1.4.2)$$

where $f_2(L) \to 0$ as L, the sample size (measured in units of the lattice constant) approaches infinite. c_1 and c_2 are constants, and t and ν are the critical exponents for electrical conductivity and correlation length respectively. Note that the system size length L is the distance across which a voltage is applied on the sample. For an infinite sample, the correcting higher order terms in equation (1.4.2) disappear and the equation reduces to

$$\sigma = c_1 L^{-t/\nu}. \qquad (1.4.3)$$

It is clear from equation (1.4.3) that a natural-log plot can give a plausible estimate of t/ν and hence the value of t from the known value of ν. The value ν has been evaluated exactly from scaling laws as 4/3.

Using Monte Carlo simulation, Lobb et al. [22] found $t/\nu = 0.973 \pm {}^{0.005}_{0.003}$, on a square lattice of resistors and $t = 1.297 \pm {}^{0.007}_{0.004}$, which is comparable to Zabolitzky's [23] result of $t/\nu = 0.973 \pm 0.005$.

Zabolitzky calculated the conductivity of a random network of resistors in two dimensions. The relation between the critical exponent for conductivity t, and other critical exponents of percolation from scaling assumptions [3] takes the form

$$t/\nu = 3d/2 - 2 - \beta/2\nu. \qquad (1.4.4)$$

Equation (1.4.4) is the Alexander-Orbach rule. Taking the scaling values of $\nu = 4/3$ and $\beta = 5/36$, $t/\nu = 0.9479$ which is in disagreement to the values of Lobb et al. [22] and Zabolitzky [23] in two dimensions. However, it has been argued that equation (1.4.4) is valid only for dimensions d higher than six [3,9]. The reason is that, transport properties on a percolating network involves both the randomness of the diffusion process of the particles and the randomness of the percolating network itself.

CHAPTER TWO. EXPERIMENTAL TECHNIQUES

2.1 THE AMMETER-VOLTMETER METHOD.

In all the four common lattices considered, i.e square, triangular, kagome' and honeycomb lattices, we have used the Voltmeter-Ammeter method as shown in fig.2.1.1. In this method, a d.c current source or d.c voltage source ε is connected in series with an Ammeter A and the resistor R, and the voltmeter is connected across the resistor. The arrangement in fig.2.1.1 demands that the voltmeter has very high input impedance so that very little or no current is drawn into the meter. It also requires that the Ammeter is of low resistance such that the current passing through the Ammeter is essentially the same through the resistor as well. In other words, there should be negligible potential drop across the Ammeter. In our case, the resistance of the digital voltmeter used was much larger than the resistance of the resistor R, hence any small currents drawn by the meter were negligible. However, the potential drop across the resistor had an

additional potential drop due to the connecting cables. This had to be subtracted in all the calculations.

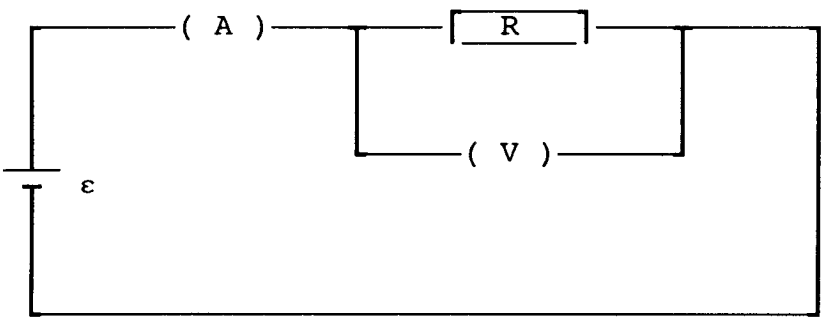

Fig.2.1.1 Ammeter-voltmeter method

The macroscopic quantities of voltage V, current I and resistance R are of primary interest when one is making electrical measurements on real conducting objects. They are the quantities that one simply reads on meters. The resistance R of a resistor is related to the voltage V applied across the resistor and the resultant current flow I, passing through the resistor by the

Ohm's law;

$$V = IR \cdot \qquad (2.1.1)$$

The value of the resistance to be a useful circuit component, it must remain fairly constant over a wide range of voltages and currents. We call the device Ohmic if it satisfies the above criterion. There are however many circuit uses for non-Ohmic components but not as resistors. We shall confine ourselves to Ohmic circuits only. The resistance must also remain fairly constant for long periods of time and must not change greatly with temperature to have Ohmic characteristics. Metals have excellent properties which make them usable in Ohmic circuits, and it is for this reason that we have used Aluminium foil as our resistive material throughout our experiments.

2.2 CONDUCTIVITY OF AN ALUMINIUM FOIL

The resistance of a rectangular conducting foil (sheet of aluminium) of length l, width w and thickness d is given in most under-graduate textbooks by the standard relationship as

$$R = \rho \frac{l}{wd} , \qquad (2.2.1)$$

where ρ is the resistivity of the material which is characteristic of the material and increases with increasing temperature. Considering a square foil where the length l equals the width w, equation (2.2.1) reduces to

$$R = \rho \frac{1}{d} . \qquad (2.2.2)$$

The electrical conductivity σ of a material is given as the reciprocal of the resistivity as

$$\sigma = \frac{l}{Rwd} , \qquad (2.2.3)$$

and for a square material, we have

$$\sigma = \frac{1}{Rd} \ . \qquad (2.2.4)$$

Thus, knowing the resistance R of a square or any rectangular aluminium foil from Ohm's law, eq. (2.1.1) and measuring the thickness d, one can calculate the conductivity of the foil. Interestingly, the conductivity σ is independent of the dimensions of the square and is only a function of sheet thickness, material, and structure. It is expressed as follows, $[\sigma] = (\Omega m)^{-1}$.

2.3 SAMPLE PREPARATION AND MATERIALS

The general experimental setup was topologically similar to the experiments of Last and Thouless [17] and Watson and Leath [18] for all the four common lattices considered. A sheet of aluminium foil was purchased from a local shop measuring 45cm x 7m with thickness d measuring $(2.28 \pm 0.08)x10^{-2}$mm. The foil thickness was calculated from the definition of density. Since the density of aluminium was known, several square foils measuring 10cm, 15cm and 20cm were cut and their masses were obtained on an electronic balance. The error in the thickness was calculated by adding the fractional errors in the mass, length and density. Enough graph pads with square grid spacing of 2mm were purchased for both lattice drawing and plotting of the preliminary data. A 0.5 Molar solution of coppersulphate was prepared by dissolving 40 grams of coppersulphate powder in 500 cubic centimeters of distilled water. This 0.5 molar solution of coppersulphate was used in the copperplating process of the two opposite ends of the aluminium foil. The connections to the external circuit were made at these copperplated ends. The experimental procedure

and setup for copperplating process can be found in most elementary physics or chemistry textbooks. However, care was taken in cleaning the copper electrodes and the aluminium electrodes (samples) before copperplating. The copperplated ends of the aluminium foil were connected to the external circuit by soldering the connecting cables to ensure an ohmic contact. A digital, high input impedance voltmeter and a digital, low resistance Ammeter were used to measure the voltage and current respectively in all the experiments on the four different lattices. The potential drop across the resistor (sample) had an additional potential drop due to the connecting cables and this had to be subtracted in all the calculations. To reduce overheating of the aluminium (sample), the current readings were maintained well below 0.1A and the voltage below 0.015V.

2.4 CONDUCTIVITY OF A SQUARE LATTICE

A square of an aluminium foil measuring 20cm X 20cm was cut and copperplated the two opposite ends using a 0.5 molar solution of coppersulphate. From a 2mm square graph paper, we constructed a 50 x 50 square lattice by drawing a 4mm square grid, see fig. 2.4.1 on page 27. The square aluminium foil was covered by the 4mm square grid representing a square lattice with 2500 sites and the system was glued to a wooden cardboard. Finally the system was mounted onto a table where external connections were made. The two copperplated ends were soldered to the external circuit and the connections completed as shown in figure 2.1.1. A constant current power supply was used to supply known currents to the sample. Since the resistance of a metal increases with temperature, current fluctuations were maintained well below 0.3 per cent of an Amp to avoid drastic resistance changes due to rise in temperature. By passing a known current through the foil and obtaining a corresponding voltage across the foil, the resistance of the foil was calculated. A series of current and voltage values were obtained and the resistance of the foil at every

stage was calculated using the least square fit method, see appendix A1. The corresponding electrical conductivity σ for a square lattice was calculated using equation (2.2.4).

A hole punched in the foil represents a "closed" site with the probability (1-p) and the unpunched site represents an "open" site with probability (p). The holes were punched or drilled using a sharp cylindrical metal with hole diameter approximately 6mm as shown in fig. 2.4.1. The diameter of the hole was not always uniform as we kept on sharpening each time it got blunt. Since we are removing sites from the system, this becomes a site-percolation problem on a square lattice with nearest neighbour bonds being cut. The hole diameter used was larger than the size of the site so that the two nearest neighbour holes can completely cut the bond between them. This implied first and second nearest neighbour overlap and becomes a problem of overlapping circles in 2-dimensions or a problem of overlapping spheres in 3-dimensions discussed by Pike and Seagers [24]. The holes were punched randomly in the foil with the help of a table of pseudo-random numbers generated by a Fortran program shown in appendix A2 and a sample

of random numbers with a test of randomness is shown in appendix A3. The seed and other constants on the Fortran program were obtained from a table of constants in Numerical Recipes [25]. The random numbers generated were used to determine the co-ordinates of the sites to be removed. The resistance of the foil without any hole cut, was the standard resistance or the bulk value resistance or the initial value resistance R_0 and the corresponding conductivity as the bulk value conductivity σ_o. The resistance of the foil was measured approximately every after 25 pairs of random numbers neglecting the repeated co-ordinates. Due to fluctuations, we took measurements after less number of random numbers. Fig. 2.4.1 shows a photocopy of a square lattice with a fraction of the removed sites = 0.16. We continued to drill the holes in the foil until no current was registered in the Ammeter. At this stage, the foil had infinite resistance or zero conductivity. The total number of holes cut at zero current determined the percolation threshold p_c for the square lattice. A graph of the conductivity per site σ/σ_0 versus the concentration of holes (1-p) was plotted as shown in fig. 3.1.1(a).

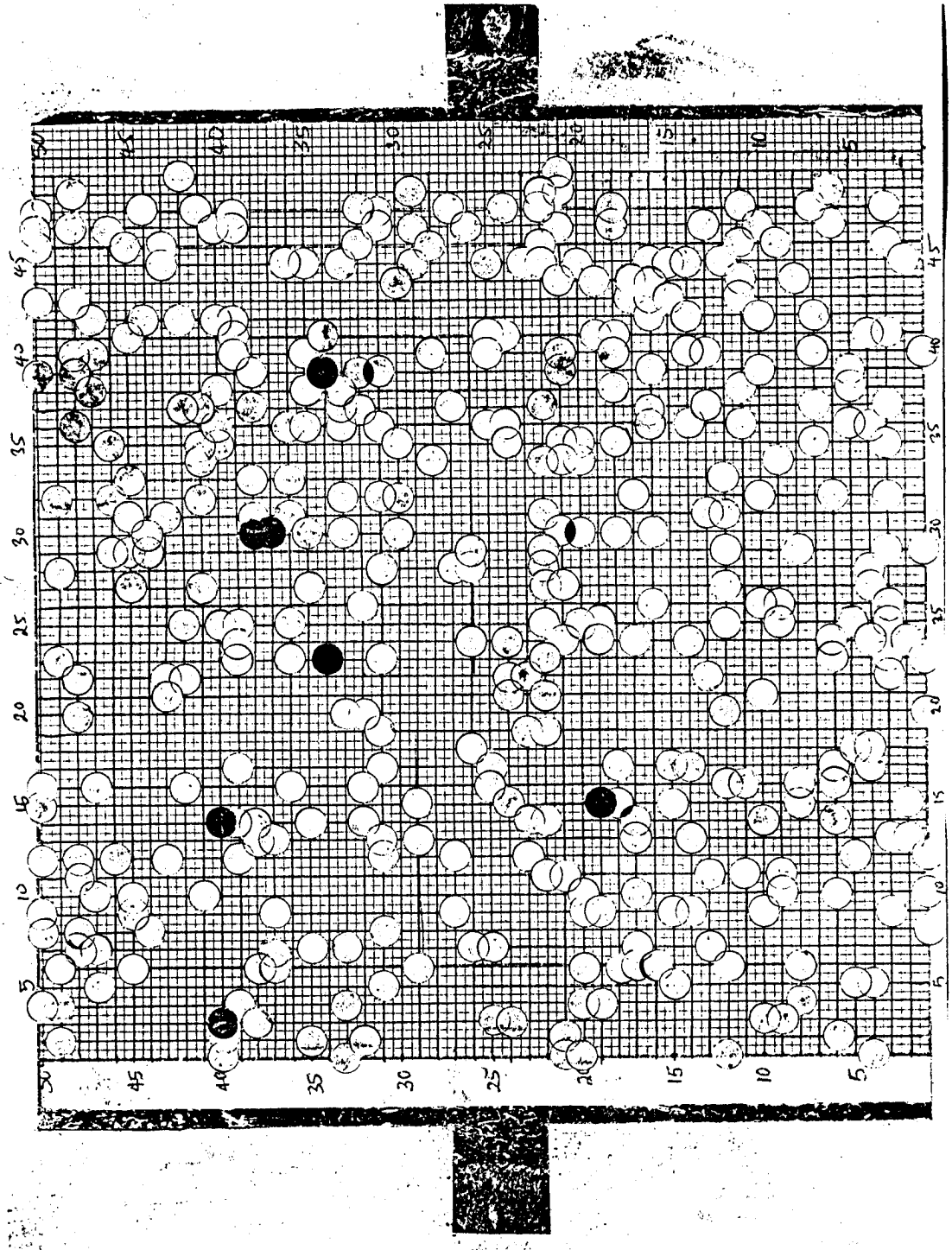

Fig.2.4.1 Photocopy of a 50 x 50 square lattice at a fraction of holes = 0.160.

2.5 CONDUCTIVITY OF A TRIANGULAR LATTICE

From a 2mm graph paper, a triangular lattice was made by drawing isosceles triangles measuring 6mm approximately. The whole triangular lattice consisted of 50 X 50 lattice points. By the geometry of this lattice, the entire system turned out to be rather rectangular in shape and not square as can be seen in fig. 2.5.1. The reason is that some points or sites on the original 2mm square grid did not make part of the triangular lattice. Due to this geometry, the total number of sites on a 50 X 50 triangular lattice reduced to 1250. Copperplated and soldered the two opposite ends of the foil as described in section 2.4 for a square lattice. Covered this triangular shape on the aluminium foil and glued the system to a wooden cardboard and external connections were made on the table. A current source power supply was used to supply known currents to the sample. By passing a known current through the foil and obtaining a corresponding voltage across the foil, the resistance was calculated. Obtained a series of current and voltage values for a given number of holes and the resistance

was calculated using the least square fit method. The electrical conductivity of the foil was calculated using equation (2.2.3).

A hole punched in the foil represents a "closed" site with a probability (1-p) and the unpunched site represents an "open" site with probability p. The holes were punched by the help of a sharp cylindrical metal with hole diameter of 6mm approximately. This impied first nearest neighbour overlap only. The second nearest neighbour overlap could not work simply because, the constrictions became so tiny that in most cases ended up breaking. In other words, the second and third nearest neighbour sites were so close to each other that, cutting the second nearest neighbour would result in cutting the third neighbour as well. The holes were drilled randomly in the foil with the help of new set of random numbers obtained by changing the seed and other constants in the Fortran program used in section 2.4. The resistance of the foil was measured approximately every after 25 pairs of of numbers. Fig. 2.5.1 on page 30, shows a photocopy of a triangular lattice with concentration of holes equal to 0.176. The holes were punched until no conduction was

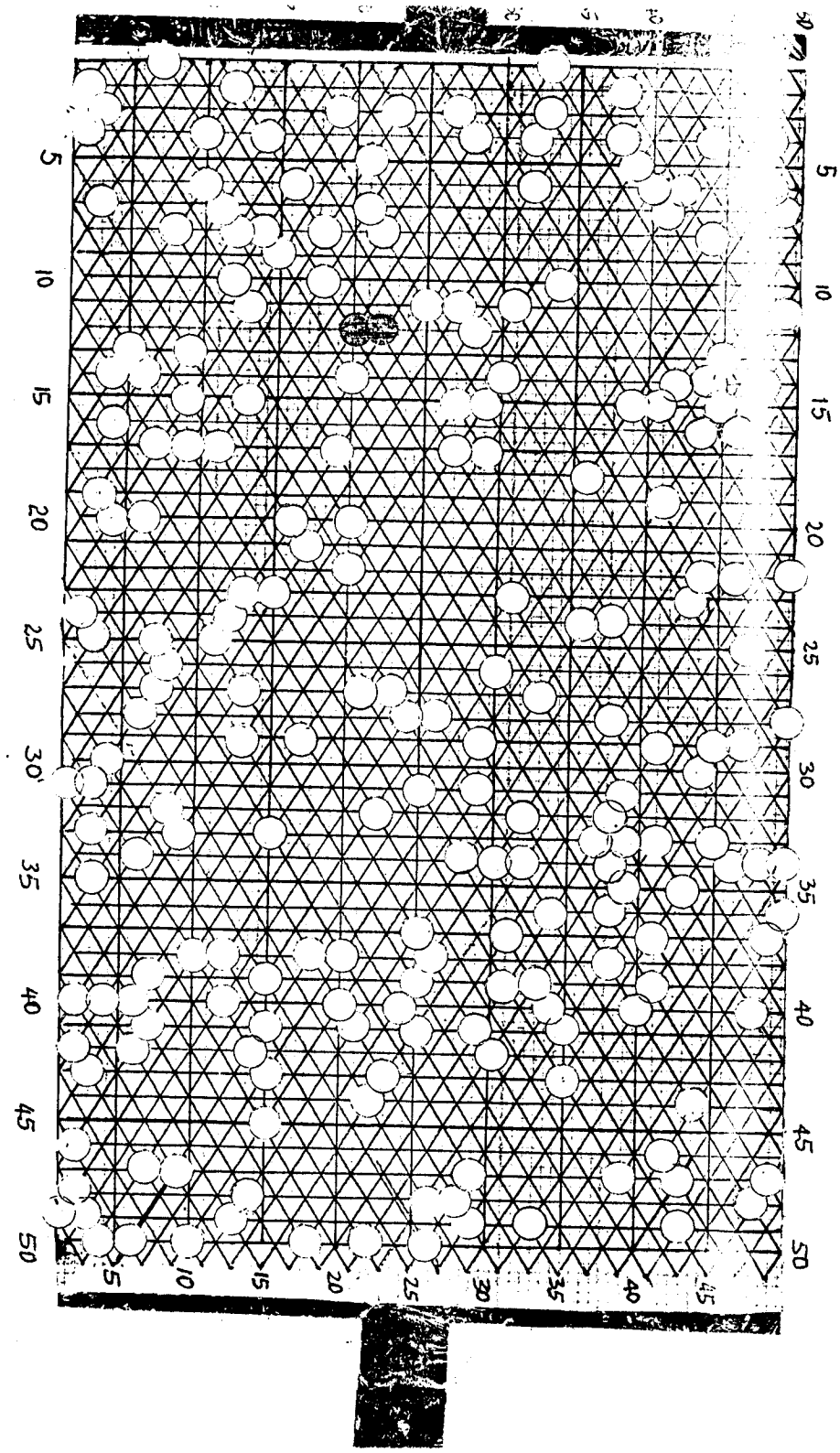

Fig.2.5.1 Photocopy of a 50 x 50 triangular lattice at a fraction of holes = 0.176.

observed through the foil. A graph of electrical conductivity per site versus the concentration of holes was plotted as shown in fig. 3.1.1(b).

2.6 CONDUCTIVITY OF A HONEYCOMB LATTICE

4mm honeycomb lattice was constructed on a 2mm square graph paper such that the whole lattice consisted of 50 X 50 sites. From the geometry of this lattice, see fig. 2.6.1, some of the sites on the graph paper could not constitute the honeycomb lattice. These sites had to be subracted from the total number of sites and now the entire lattice had 1250 sites. The honeycomb lattice was covered on an aluminium foil and pasted onto it. The two opposite ends of the foil were copperplated and soldered to the external circuit as done for the square lattice explained in section 2.4. The system was glued on a wooden cardboard and mounted on a table where external connections were made.

A hole punched in the foil represents a "closed" site with a probability (1-p) and the undrilled site represents an "open" site with probability (p). A hollow cylindrical metal of diameter 6mm was used to drill the holes in the foil. This was a site-percolation problem with first and second nearest neighbour overlap. The holes were punched with the help of pseudo-random numbers generated by a new seed and constants to determine the co-ordinates. The resistance of the foil was measured every after 25 pairs of numbers neglecting the repeated co-ordinates. We drilled the holes in the honeycomb lattice until no current was registered in the Ammeter. Fig 2.6.1 on page 33, shows the honeycomb lattice photocopied at the concentration of removed sites of 0.152. From the total number of holes cut at zero conductivity, we were able to calculate the percolation threshold for the honeycomb lattice. The conductivity of the honeycomb lattice was calculated from equation (2.2.4). A plot of the conductivity per unity site versus the concentration of holes (1-p) for the honeycomb lattice was made as shown in fig. 3.1.1(c).

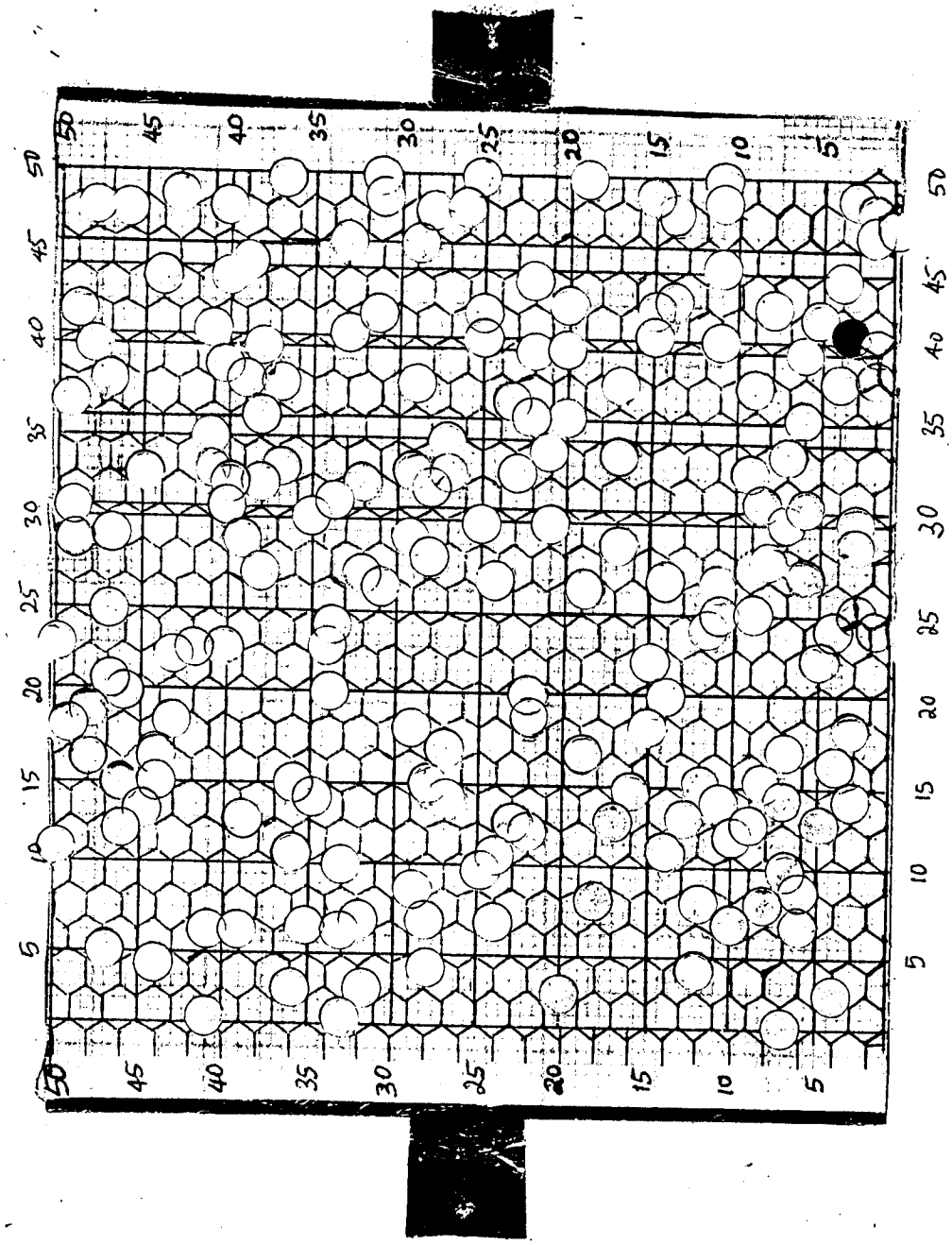

Fig.2.6.1 Photocopy of a 50 x 50 honeycomb lattice at a fraction of holes = 0.152.

2.7 CONDUCTIVITY OF A KAGOME' LATTICE.

A two millimeter graph paper was used to make a kagome' lattice measuring six millimeter as shown in fig 2.7.1. It was easier to construct a 6mm lattice than a 4mm one, considering only first and second nearest neighbours. The kagome' lattice consisted of a 50 X 50 lattice and due to the geometry of the lattice, some of the sites on the graph paper could not make part of the kagome' lattice and the whole array of points formed a rectangular shaped lattice instead of a square, see fig. 2.7.1 page 36. These sites had to be neglected when determining the site to be removed or when deciding the hole to be punched. The total number of sites that made up the entire kagome' lattice was now 938. The kagome' lattice was now glued to the aluminium foil whose two opposite ends had been copperplated. The system was glued onto a wooden cardboard and then mounted on a table where external connections were completed. The connecting cables were soldered on the copperplated ends to ensure an ohmic contact. Using a current power supply, a known current was passed through the foil and a corresponding voltage was

obtained. A series of currents and voltages were obtained for a given number of holes and a least square fit method was used to determine the resistance of the kagome' lattice.

A site removed from the lattice by punching a hole in the foil represents a "closed" site with a probability (1-p) and an unremoved site represents an "open" site with a probability (p). A sharp hollow cylindrical metal of diameter 10mm was used to drill holes in the foil. Similarly, this was a site-percolation problem as we were removing sites from the system with first and second nearest neighbour overlap as seen in section 2.4 for the square lattice. Holes were punched randomly by the help of pseudo-random numbers to determine the co-ordinates. Fig. 2.7.1 shows a photocopy of a kagome' lattice at a concentration of holes equal to 0.23. The resistance of the foil was calculated after every 25 pairs of numbers using the least square fit method. Note that near percolation threshold resistance was calculated after fewer holes than 25. The conductivity was calculated using eq.(2.2.3). Holes were punched until no current passed through the foil. At this stage, the percolation threshold for the kagome' lattice was determined.

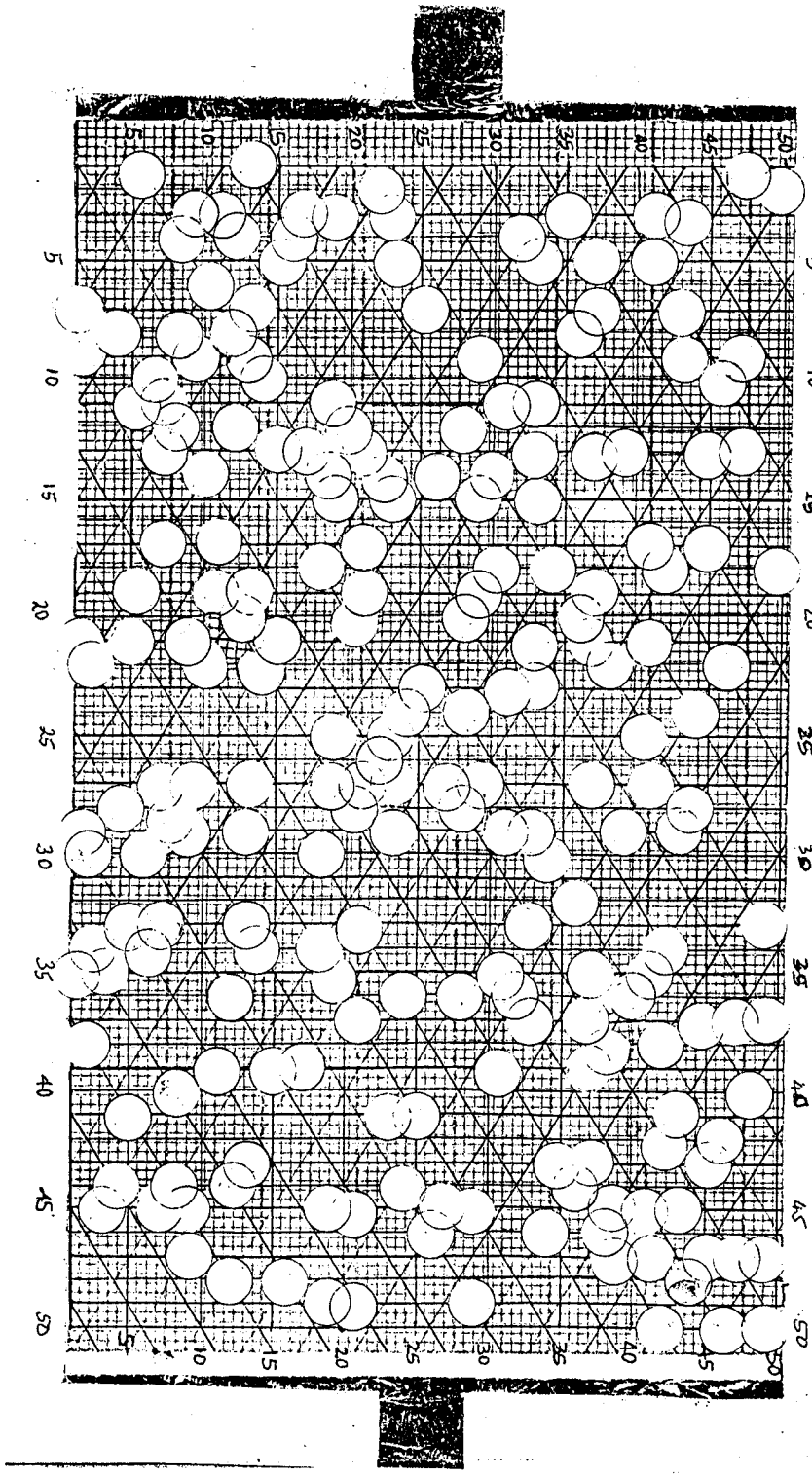

Fig.2.7.1 Photocopy of a 50 x 50 Kagome' lattice at a fraction of holes = 0.23.

CHAPTER THREE RESULTS

3.1 THRESHOLD PARAMETER p_c

The resistance of the aluminium foils increased as the number of holes punched increased. In other words, the conductivity of the foils reduced as the number of holes punched increased. The reason was that, by punching holes in the foils reduced the number of conducting channels or conducting paths as most of these channels were being cut and hence reduced the conductivity.

The experimental determination of the percolation threshold values p_c was very straight forward. The total number of holes punched at zero conductivity could easily be counted and since the fraction of holes cut is given by (1-p), then percolation threshold could be determined. However, the estimate of p_c had some inherent errors which were mostly statistical or random errors. For example the random numbers used to locate the co-ordinates were not absolutely random. We tried to minimize these statistical errors by taking repeated measurements. The errors in the values of p_c

were determined by subtracting the p_c value obtained by a set of random numbers from another p_c value obtained by a different set of random numbers. Note that the fraction of holes (1-p) was taken to be equal to the number of holes and ignored the overlap. This contributed to the systematic errors.

On a 50 x 50 square lattice, the value of p_c was found to be 0.57 ± 0.04, which is close to the estimate of 0.59 for the critical proportion of open sites for this problem. The results of the experiment are shown in table 3.1.1 on page 39, which is a table showing the number of holes cut, the conductivity and the fraction of holes. The conductance became zero when there were no conducting channels across the foil and for a square lattice it occurred at the concentration of holes equal to 0.43. Figure 3.1.1(a) shows a plot of the ratio of the conductivity of the square foil to its initial value σ/σ_o versus the concentration of holes (1-p). Since the percentage errors in the conductivity were known, the absolute errors in the ratio of the conductivity were calculated *by adding the percentage errors.*

Table 3.1.1. Values of the number of holes, the conductivity and the fraction of holes for square lattice.

holes cut	σ/σ_o	1-p
zero	1.000±0.674	0.000
25	0.648±0.438	0.010
50	0.318±0.215	0.020
200	0.294±0.199	0.080
275	0.132±0.091	0.110
475	0.190±0.128	0.190
600	0.156±0.105	0.240
675	0.132±0.090	0.270
700	0.125±0.084	0.280
725	0.114±0.077	0.290
800	0.092±0.062	0.320
825	0.091±0.061	0.330
875	0.076±0.052	0.350
925	0.063±0.043	0.370
950	0.056±0.038	0.380
975	0.035±0.023	0.390
1025	0.030±0.020	0.410
1050	0.028±0.018	0.420
1074	0.000±0.000	0.430

For the triangular lattice, the value of p_c was found to be 0.525 ± 0.035 which is comparable to the simulated and power series value given in [8] as 0.50 and in [4] as 0.50. The data for this lattice is

shown in table 3.1.2 below and the gragh of the conductivity per site versus the fraction of holes is shown in fig.3.1.1(b) on page 43. All the conducting channels were cut at a concentration of holes equal to 0.475.

Table 3.1.2 shows the number of holes, conductivity and the fraction of holes for a triangular lattice.

holes cut	σ/σ_o	(1-p)
zero	1.00±0.699	0.000
100	0.821±0.571	0.080
161	0.450±0.312	0.128
220	0.373±0.260	0.176
360	0.309±0.215	0.288
421	0.218±0.151	0.337
440	0.171±0.119	0.352
500	0.146±0.101	0.400
510	0.144±0.100	0.408
521	0.072±0.050	0.417
530	0.071±0.049	0.425
551	0.054±0.038	0.441
560	0.051±0.036	0.448
565	0.047±0.033	0.452
570	0.045±0.031	0.456
585	0.044±0.030	0.468
590	0.043±0.029	0.472
594	0.000±0.000	0.475

For the 50 x 50 honeycomb lattice, the last conducting channel of the system was cut when the fraction of holes (1-p) was 0.303. This gave the value of p_c as 0.697 ± 0.007 which is comparable to the value of 0.70 by [8]. The results of the experiment are shown in table 3.1.3 and the plot of the ratio of the conductivity of the foil to its initial value versus the fraction of holes (1-p) for a honeycomb lattice is shown in fig. 3.1.1(c).

Table 3.1.3 shows the number of holes, conductivity and the fraction of holes cut for honeycomb lattice.

holes cut	σ/σ_o	(1-p)
zero	1.630±0.700	0.000
100	0.397±0.274	0.080
190	0.293±0.203	0.150
253	0.216±0.152	0.200
273	0.175±0.122	0.220
300	0.163±0.113	0.240
320	0.141±0.098	0.256
325	0.118±0.106	0.260
335	0.106±0.075	0.268
345	0.076±0.052	0.276
350	0.073±0.051	0.280
365	0.066±0.046	0.292
370	0.063±0.043	0.296
375	0.031±0.021	0.300
377	0.028±0.019	0.302
379	0.000±0.000	0.303

For the 50 x 50 kagome' lattice, the zero conductivity was witnessed at the concentration of holes (1-p) equal to 0.374. This gave the value of the percolation threshold p_c as 0.626 ± 0.084 comparable to the value of 0.65 given by [8]. Table 3.1.4 shows results obtained for the kagome' lattice and these results are plotted in fig. 3.1.1(d), which is a plot of the normalised conductivity against the concentration of holes.

Table 3.1.4 showing the number of holes cut, the conductivity and the fraction of holes for kagome' lattice.

holes cut	σ/σ_o	(1-p)
zero	1.000±0.683	0.000
57	0.406±0.276	0.061
160	0.365±0.250	0.171
230	0.188±0.128	0.245
240	0.174±0.119	0.256
250	0.128±0.088	0.266
272	0.087±0.059	0.290
290	0.082±0.057	0.309
301	0.078±0.053	0.320
310	0.053±0.036	0.330
324	0.046±0.031	0.345
330	0.043±0.029	0.350
341	0.0169±0.0116	0.364
348	0.0167±0.0113	0.371
350	0.0164±0.0112	0.373
351	0.0000±0.0000	0.374

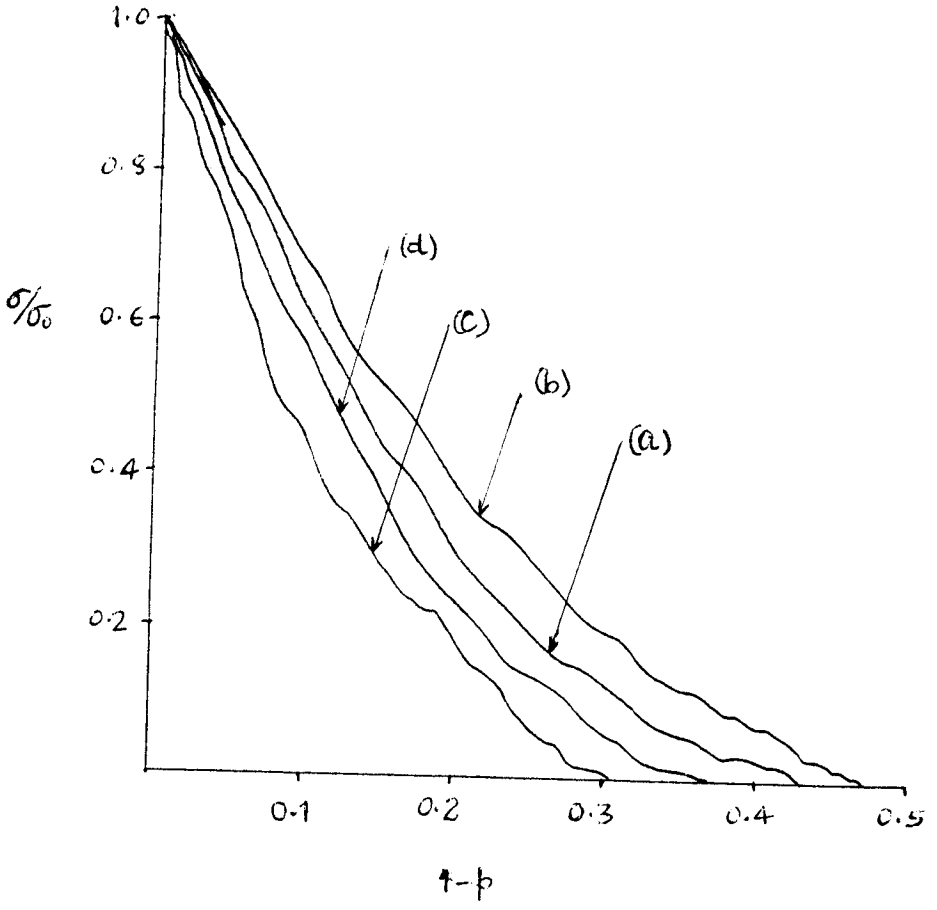

Fig. 3.1.1 Graph of the conductivity as a function of the fraction of holes for (a) square, (b) triangular, (c) honeycomb and (d) kagome' lattices.

From the foregoing, the variability of the percolation threshold p_c from lattice to lattice has been confirmed. We further calculated the critical area fraction ϕ_c for our site-percolation problem, which is the product of the filling factor v for the lattice and the percolation threshold p_c i.e, $\phi_c = vp_c^{site}$. The filling factor is defined as the fraction of the total area filled by circles. Using the values of v from [8] and the experimentally obtained values of p_c, we find ϕ_c values a remarkable insensitivity to lattice structure as shown in table 3.1.5 below. The critical area fraction in 2-dimensions is 0.45.

Table 3.1.5 shows the lattice type, experimental values of the percolation threshold, the filling factor and the critical area fraction.

lattice type or structure	p_c^{site}	filling factor v	vp_c^{site}
square	0.57	0.7854	0.45
triangular	0.525	0.9069	0.48
honeycomb	0.697	0.6046	0.42
kagome'	0.626	0.6802	0.43

3.2 ESTIMATE OF THE CRITICAL EXPONENT t

It is known that conductivity fluctuations in a finite sample are larger near the percolation threshold i.e within the critical region. The complexity nature of these fluctuations make it difficult to determine experimentally the onset of these fluctuations. We can roughly estimate the fluctuation range by using the scaling arguments mentioned in sect.1.3 i.e, by assuming that the correlation length becomes comparable to the system size length, (c.f. eq.(1.3.3)).

One of the most important quantities in the estimate of the critical exponent t is the concentration of sites (p). Since the concentration of holes (removed sites) is not directly proportional to the number of holes due to the allowed overlap, we had to use the lattice percolation formula suggested by Pike and Seagers [24]. In that case, the foil area fraction p for our systems in 2-dimensions then become

$$p = \exp[-n\pi r^2/s], \qquad (3.2.1)$$

where r is the radius of the holes, n is the number of

holes and s the sample area. We can generalise from eq. (1.4.1) that $\sigma/\sigma_0 \sim |p-p_c|^t$, and taking natural-log gives $\ln(\sigma/\sigma_0) \sim t \ln|p-p_c|$ and a slope of this latter expression gives a rough estimate of t. The critical exponent t was calculated using the least square fit method. We calculated the χ^2_m(Chi-square) for each lattice per degree of freedom m for the least square fit method. We define m = n-g where n is the number of data points and g = 2 for straight line fit. In the calculations of $|p-p_c|$, we obtained the value of p from eq.(3.2.1) since the values of the radius r, sample size s and the number of holes cut n are known for each lattice. We however used the experimentally determined value of p_c in the calculations of $|p-p_c|$.

Table 3.2.1 shows the results for the 70 x 70 square lattice with 4mm lattice and 6mm hole diameter. The radius r=3mm and sample area s=115600mm^2 and the p_c experimental was 0.51. Fig. 3.2.1 shows a typical natural-log plot of the normalised conductivity as a function of $|p-p_c|$ for a square lattice. The value of t was found to be 1.42 ± 0.48 and χ^2_5 = 1.45. The error in the $\ln(\sigma/\sigma_0)$ was calculated as follows;
Define $Q = \ln(\sigma/\sigma_0)$. The error in Q is given by

$\delta Q = \frac{dQ}{d(\sigma/\sigma_0)} \delta(\sigma/\sigma_0)$, where $\delta(\sigma/\sigma_0)$ is the uncertainty.

But $dQ/d(\sigma/\sigma_0) = 1/(\sigma/\sigma_0)$. Hence the error in Q will be given by $\delta(\sigma/\sigma_0)/(\sigma/\sigma_0)$.

Table 3.2.1 shows values of the conductivity within the critical region for square lattice.

holes cut	σ/σ_o	$\lvert p-p_c \rvert$	$\ln\lvert p-p_c \rvert$	$\ln(\sigma/\sigma_o)$
2175	0.122±0.094	0.077	-2.56	-2.10±0.77
2200	0.118±0.081	0.074	-2.60	-2.14±0.69
2215	0.074±0.052	0.072	-2.63	-2.60±0.70
2240	0.067±0.046	0.068	-2.69	-2.70±0.69
2300	0.065±0.044	0.060	-2.81	-2.73±0.68
2325	0.063±0.043	0.056	-2.88	-2.76±0.68
2380	0.060±0.041	0.049	-3.02	-2.81±0.68

For the triangular lattice, table 3.2.2 shows a display of results for a 50 x 50 triangular lattice with 6mm lattice and 6mm hole diameter. Fig. 3.2.2 shows the natural-log plot of the normalised conductivity as a function of the $|p-p_c|$ for r = 3mm and s = 39932mm^2. The value of the slope t was equal to 1.42 ± 0.44 close to predicted value of the critical exponent t for the two-dimensional lattice. The value of χ^2_3 = 2.30 and 3 being the degree of freedom.

For the triangular lattice, table 3.2.2 shows a display of values for the conductivity within the critical region.

holes cut	σ/σ_o	$\lvert p-p_c\rvert$	$\ln\lvert p-p_c\rvert$	$\ln(\sigma/\sigma_o)$
560	0.0513±0.0355	0.148	-1.91	-2.97±0.69
565	0.0473±0.0327	0.145	-1.93	-3.05±0.69
570	0.0454±0.0312	0.143	-1.94	-3.09±0.69
585	0.0438±0.0304	0.138	-1.98	-3.12±0.69
590	0.0436±0.0299	0.134	-2.01	-3.13±0.68

Table 3.2.3 shows values of the conductivity within the critical region for the 50 x 50 honeycomb lattice with 4mm lattice and 6mm hole diameter. Fig.3.2.3 shows a typical natural-log plot of the normalised conductivity as a function of $|p-p_c|$ for radius of 3mm and sample area of 33735mm^2. The slope t from best fit was 1.73±0.18. The value of p_c experimental was 0.697 ± 0.007 and the χ^2_9 as 0.74.

Table 3.2.3. Values of the conductivity within the critical region for honeycomb lattice

holes cut	σ/σ_o	$\lvert p-p_c\rvert$	$\ln\lvert p-p_c\rvert$	$\ln(\sigma/\sigma_o)$
253	0.175±0.122	0.098	-2.32	-1.74±0.70
273	0.163±0.113	0.081	-2.51	-1.81±0.69
300	0.141±0.098	0.068	-2.69	-1.96±0.70
320	0.118±0.084	0.065	-2.73	-2.14±0.71
325	0.106±0.075	0.058	-2.85	-2.24±0.71
345	0.076±0.052	0.052	-2.96	-2.58±0.68
350	0.073±0.051	0.049	-3.02	-2.62±0.70
365	0.066±0.046	0.046	-3.08	-2.71±0.70
370	0.063±0.043	0.039	-3.24	-2.77±0.68
375	0.031±0.021	0.036	-3.32	-3.49±0.68
377	0.028±0.019	0.033	-3.41	-3.58±0.68

From the constructed 6mm lattice of the 50 x 50 kagome' lattice and 10mm hole diameter, we calculated the area of the resulting system as 40500mm^2 and hole radius as 5mm. Table 3.2.4 shows values of the conductivity for a kagome' lattice within the critical region, the value of p_c obtained from the formula was 0.507 and using the values of p from page 42, we completed table 3.2.4. The value of the slope from the best fit straight line was 3.16 ± 0.19 and the value of chi-squared with eleven degrees of freedom was equal to 0.91. This value seems larger than expected and the explanation may be that, the effective number of sites considered were very few as we had to neglect those sites that did not make part of the kagome' lattice, see page 34.

Table 3.2.4. Values of the conductivity within the critical region for kagome' lattice.

holes cut	σ/σ_o	$\lvert p-p_c \rvert$	$\ln\lvert p-p_c \rvert$	$\ln(\sigma/\sigma_o)$
160	0.365±0.250	0.322	-1.13	-1.01±0.68
230	0.188±0.128	0.248	-1.39	-1.67±0.68
240	0.174±0.119	0.237	-1.44	-1.75±0.68
250	0.128±0.088	0.227	-1.48	-2.06±0.69
272	0.087±0.059	0.203	-1.59	-2.44±0.68
290	0.082±0.057	0.184	-1.69	-2.50±0.70
301	0.078±0.053	0.173	-1.75	-2.55±0.68
310	0.053±0.036	0.163	-1.81	-2.94±0.68
324	0.046±0.031	0.148	-1.91	-3.08±0.67
330	0.043±0.029	0.143	-1.94	-3.15±0.67
341	0.017±0.012	0.129	-2.05	-4.08±0.70
348	0.0167±0.0113	0.122	-2.10	-4.09±0.68
350	0.0164±0.0112	0.120	-2.12	-4.11±0.68

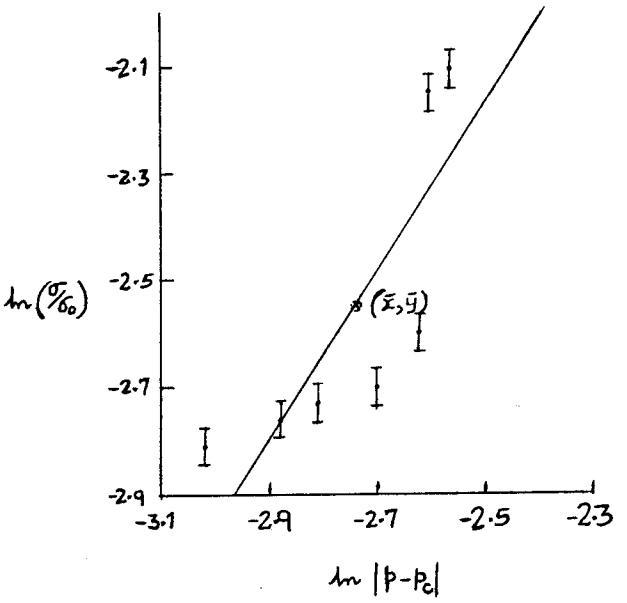

Fig. 3.2.1 Plot of $\ln(\sigma/\sigma_0)$ versus $\ln|p-p_c|$ for square lattice.

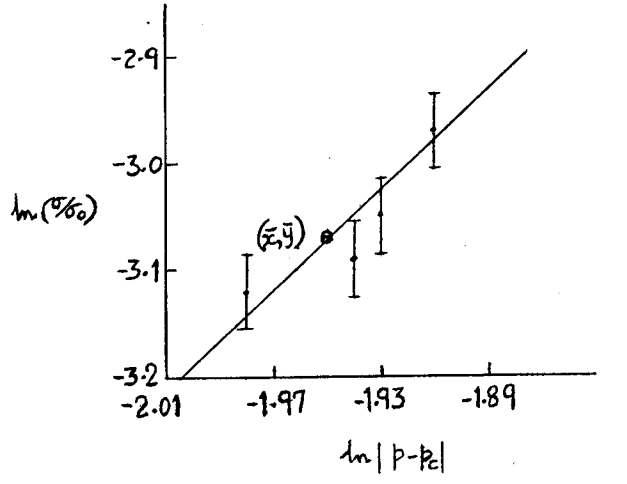

Fig. 3.2.2 Plot of $\ln(\sigma/\sigma_0)$ versus $\ln|p-p_c|$ for triangular lattice.

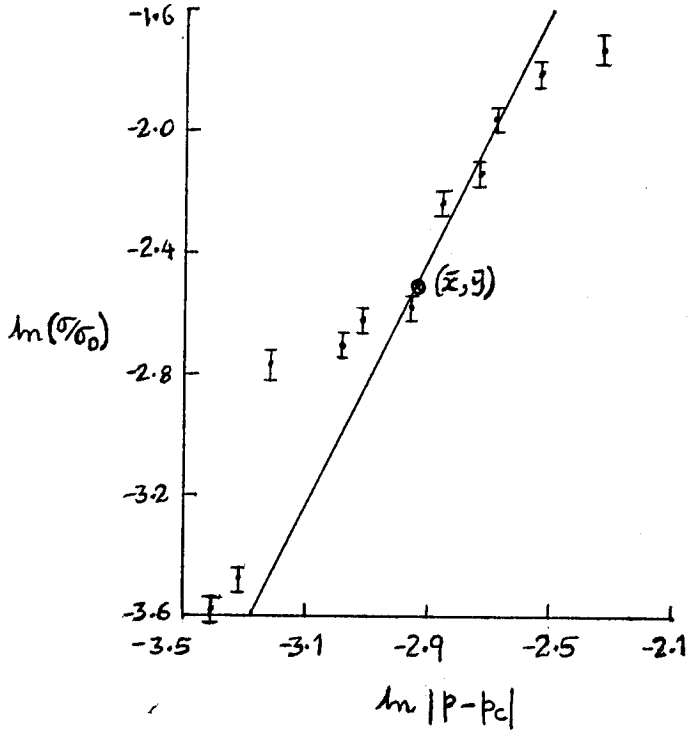

Fig. 3.2.3 Plot of $\ln(\sigma/\sigma_0)$ Versus $\ln|p-p_c|$ for honeycomb lattice.

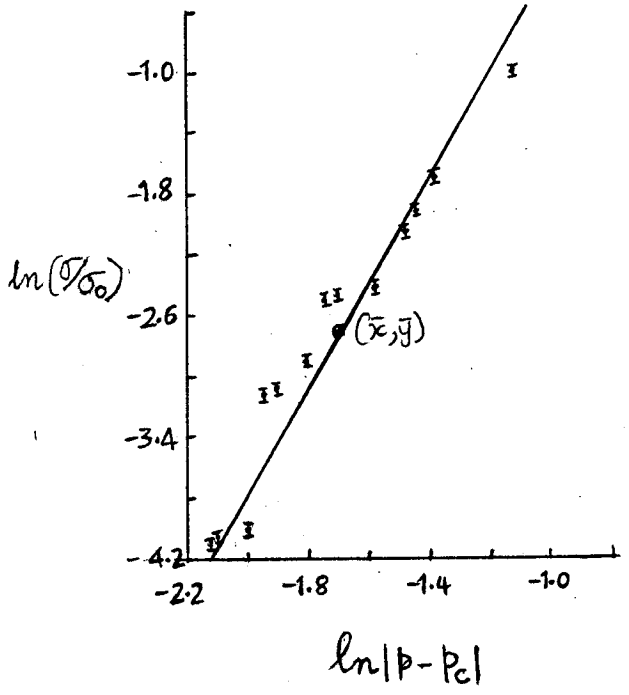

Fig. 3.2.4 Plot of $\ln(\sigma/\sigma_0)$ Versus $\ln|p-p_c|$ for Kagome' lattice.

3.3 ESTIMATE OF t/ν.

The system size lengths used for the triangular, honeycomb and kagome' lattices were 30cm, 50cm and 60cm whilst for the square lattice, we used lengths of 30cm, 50cm and 70cm. For all these dimensions, we analysed the results for each lattice for the conductivity just before the percolation threshold p_c.

For square lattice, we plotted a natural-log of the normalized conductivity as a function of the system size length and obtained the slope $-t/\nu = -1.48 \pm 0.04$, see fig. 3.3.1. Table 3.3.1 below shows a table of results for square lattice.

Table 3.3.1. Values of the conductivity and size length for square lattice.

$\sigma/\sigma_o \times 10^{-3}$	$L \times 10^{-3}$ m	ln(L)	$\ln(\sigma/\sigma_o)$
60.4±4.2	30	-3.51	-2.81±0.07
27.6±1.9	50	-3.00	-3.59±0.07
11.9±0.8	70	-2.66	-4.06±0.07

Table 3.3.2 shows results the triangular lattice and fig. 3.3.2 shows a natural-log plot of the conductivity as a function of the systen size length L. The value of the slope $-t/\nu$ from the best fit was -0.966 ± 0.725.

Table 3.3.2. Values of the conductivity and size length for triangular lattice.

$(\sigma/\sigma_o)x10^{-3}$	$Lx10^{-3}m$	ln(L)	$\ln(\sigma/\sigma_o)$
49.5±3.4	30	-3.51	-3.01±0.07
43.5±3.0	50	-3.00	-3.13±0.07
22.0±1.5	60	-2.81	-3.82±0.07

Table 3.3.3 shows results for a honeycomb lattice and fig. 3.3.3 shows a plot of the conductivity as a function of the system size length L. The slope of the straight line $-t/\nu = -1.57 \pm 0.82$.

Table 3.3.3. Values of the conductivity and size length for honeycomb lattice.

$(\sigma/\sigma_o)x10^{-3}$	$Lx10^{-3}m$	ln(L)	$\ln(\sigma/\sigma_o)$
40.8±2.8	30	-3.51	-3.20±0.07
27.9±1.9	50	-3.00	-3.58±0.07
11.7±0.8	60	-2.81	-4.45±0.07

Table 3.3.4 shows results for the kagome' lattice and fig. 3.3.4 shows a plot of the conductivity as a function of the system size length L. The value of the slope $-t/\nu$ was found to be -2.17 ± 0.17.

Table 3.3.4 showing the conductivity and the size length for kagome' lattice.

$(\sigma/\sigma_o)x10^{-3}$	$Lx10^{-3}m$	ln(L)	$\ln(\sigma/\sigma_o)$
104.0±7.2	30	-3.51	-2.26±0.07
25.2±1.7	50	-3.00	-3.68±0.07
14.9±1.0	60	-2.81	-4.21±0.07

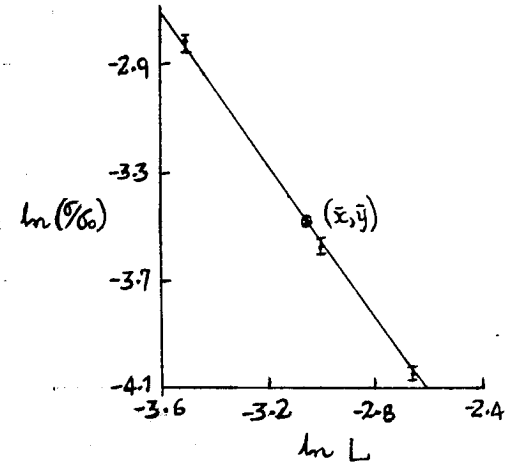

Fig. 3.3.1 Plot of $\ln(\sigma/\sigma_0)$ versus $\ln L$ for square lattice.

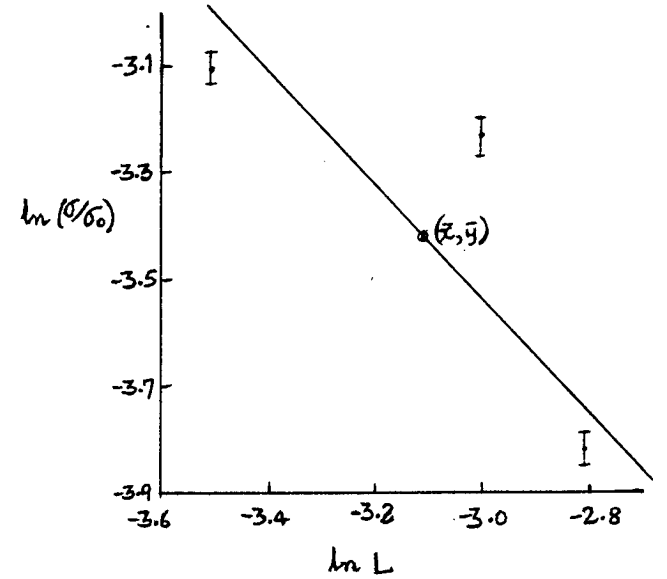

Fig. 3.3.2 Plot of $\ln(\sigma/\sigma_0)$ versus $\ln L$ for triangular lattice.

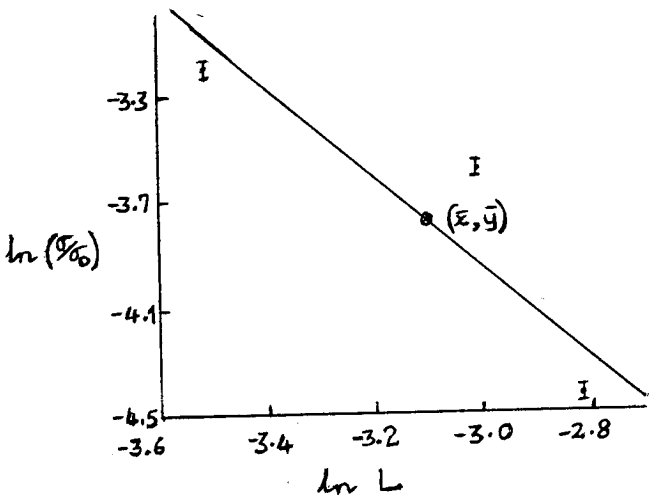

Fig. 3.3.3 Plot of $\ln(\sigma/\sigma_0)$ versus $\ln L$ for honeycomb lattice.

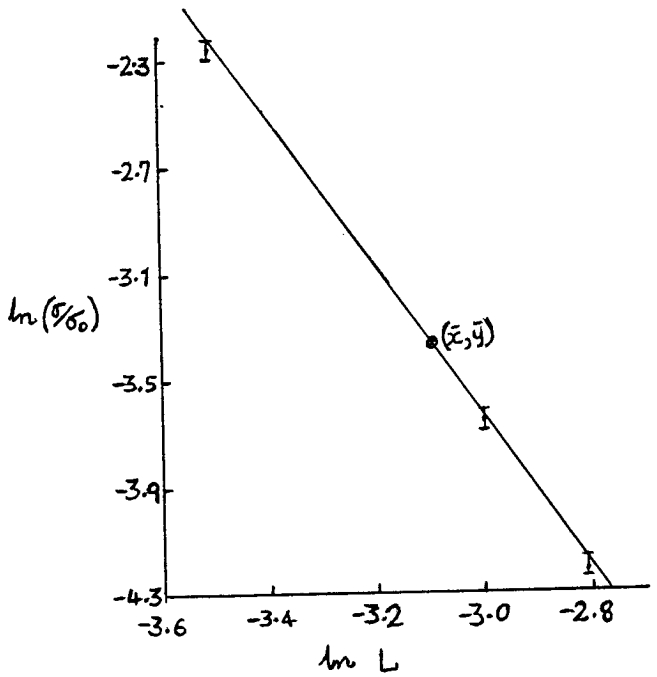

Fig. 3.3.4 Plot of $\ln(\sigma/\sigma_0)$ versus $\ln L$ for Kagomé lattice.

The data points in fig. 3.2.1, fig. 3.2.3, fig. 3.3.2, and fig. 3.3.3 seems to fall off the best fit straight line. Since we had no criteria to reject these data points, we maintain the data points as valid.

We summarise the values of the critical exponent t and the values of t/ν for the four geometrical lattices considered as shown in table 3.3.5.

Table 3.3.5 Table of the critical exponent t and the value of t/ν .

Lattice	t	t/ν
square	1.420±0.480	1.480±0.040
triangular	1.420±0.440	0.996±0.725
honeycomb	1.730±0.180	1.570±0.820
kagome'	3.160±0.190	2.170±0.170

CHAPTER FOUR CONCLUSION

The results of the preceding sections can be summarized by noting that this classical model of percolation shows critical behaviour in the onset of percolation and that the associated details of the critical region are very general in nature for each dimension and can be quantitatively understood. The dimensional invariants (critical exponents) and the percolation thresholds obtained are in good agreement with the available numerical data, and permit extension of the quantitative predictions of the theory to lattices not yet studied as well as to more general situations such as the amorphous materials.

We have verified that each of the four common two-dimensional geometrical lattices (square, triangular, kagome' and honeycomb) has a unique value of the percolation threshold showing that p_c values are structure dependent. The reason is that the nature of linkages tend to differ from lattice to lattice and hence the nature of percolating network. In general, the more linkages or connectivities on a lattice, the less the percolation threshold value. We have also shown that,

within the experimental uncertainities, the values of the critical exponents for the two-dimensional lattices are the same in conformity with the universality principle of the critical exponents. However, the size of the critical region was found to vary from lattice to lattice probably due to finite size effects and the nature of the linkages associated with each lattice. Note that the range of the critical region was chosen from the values of the natural-log of the conductivity and $\ln|p-p_c|$ away from percolation threshold and gave a reasonable value of the critical exponent t. The average value of the critical exponent t for all the four lattices considered in two dimensions was found to be 1.93 ± 0.32 which is larger than the exact value of 4/3 from the scaling assumptions. But excluding the value for the kagome' lattice, the other values are in good agreement with the theoretical value.

On the other hand, the value of the critical exponent t obtained from the natural-log plot of the normalized conductivity as a function of the system size length (c.f sect. 3.3) was rather unrealistic. This is not surprising simply because the formula

used (eq. (1.4.3)) for our samples is for an infinite lattice. The correct formula to use for finite lattices is eq. (1.4.2). However, to use this formula one has to make corrections for the higher order terms in the formula and this was not possible considering a simple table-top arrangement of our experiments. Similarly, a plausible extrapolation of the data was going to be possible if we were able to obtain the slope t/ν for a given value of the system size length L. Only computer simulations could solve this problem.

Finally it is observed that, improvements to the results could be possible if one can minimise the finite size effects of the lattices by considering very large lattices. However, it becomes very difficult to manually construct and drill holes for lattices greater than 70cm x 70cm for example. Since it is very difficult to determine the onset of the critical region due to fluctuations in the conductivity, one needs to take as many measurements as possible even away from the critical region. For a large lattice, this becomes a laborious exercise.

APPENDIX

A1 Fortran program for the best fit straight line.

```
      PROGRAM BEST
*TO FIND THE BEST FIT LINE,Y=AX+B GIVEN A SET OF DATA POINTS.
      DIMENSION X(100),Y(100),C(100),D(100)
      READ(*,*)N,(X(J),J=1,N)
      READ(*,*)(Y(J),J=1,N)
      S=0.0
      Z=0.0
      P=0.0
      Q=0.0
      DO 100 J=1,N
      S=S+X(J)*Y(J)
      Z=Z+X(J)*X(J)
      P=P+X(J)
      Q=Q+Y(J)
 100  CONTINUE
      A=((N*S)-(P*Q))/((N*Z)-(P*P))
      B=((S*P)-(Q*Z))/((P*P)-(N*Z))
      WRITE(*,20) A,B
 20   FORMAT(2X,'SLOPE A IS ='E10.3,/,2X,'INTERCEPT B IS ='E10.3)
      E=0.0
      DO 200 I=1,N
      C(I)=A*X(I)+B
      D(I)=C(I)-Y(I)
      E=E+D(I)*D(I)
 200  CONTINUE
      F=(N*N*E)/((N-2)*(N*Z-P*P))
      G=(N*E*Z)/((N-2)*(N*Z-P*P))
      V=N
      H=SQRT(F/V)
      R=SQRT(G/V)
      WRITE(*,30) H,R
 30   FORMAT(2X,'ERROR IN A IS ='E10.3,/,2X,'ERROR IN B IS ='E10.3)
      STOP
      END
```

A2 Fortran program for random number generation.

```
      PROGRAM RANDOM NUMBERS
*RANDOM NUMBERS BETWEEN 1 AND 50.
      INTEGER*4 A(6000),B(6000)
      READ(*,*) N,A(1)
      IC=1283
      IA=106
      ID=6075
      DO 100 J=1,N
      K=MOD(IA*A(J)+IC,ID)
      R=FLOAT(K)/FLOAT(ID)
      B(J)=1+INT(50.*R)
      A(J+1)=K
 100  CONTINUE
      WRITE(*,60)(B(J),J=1,N)
 60   FORMAT(20(1X,I2))
      STOP
      END
```

```
                PROGRAM RANDOM NUMBERS
*TO GENERATE RANDOM NUMBERS BETWEEN 1 AND 50 AND
*THEIR FREQUENCIES.
      INTEGER*4 A(5000),F(5000),MF(20)
      READ(*,*) N,A(1)
      IC=1283
      IA=106
      ID=6075
      DO 100 J=1,N
      K=MOD(IA*A(J)+IC,ID)
      R=FLOAT(K)/FLOAT(ID)
      F(J)=1+INT(50.*R)
      A(J+1)=K
 100  CONTINUE
      K=1
      I=4
      DO 120 M=1,10
      MF(M)=0
  120 CONTINUE
      DO 250 J=1,10
      DO 200 L=1,N
      IF (F(L).GE.K.AND.F(L).LE.K+I) MF(J)=MF(J)+1
 200  CONTINUE
      K=K+I+1
 250  CONTINUE
      WRITE(*,20) (MF(N),N=1,10)
 20   FORMAT(5(2X,I3))
      STOP
      END
```

A3 Sample of random numbers and a test for their randomness.

```
J>RAND1
2500,3215
16 45 40 50 28 16 30 40  4  5 30  4 26 50 17 43 48 41  5 25
28 12 31 27 16 16 39 14 30 12  9 23 48 48 45 46 34 45  6 15
25 29 41 33 13 13 20 10 31 36 19 44 31 41  3  5 24  7  8 20
 7 40 28  2 50 48 43 40 30 30  8 25 12  5 32 39 32  1 13 37
32 31 20 26 46 33 32  5 25 50 11 45 30 12 45 22  8 23 27 50
31 44 38 17 23 21 32 14 50 26 18 24 48 33 44 50 11  9 31  2
20 40  4 27 28 19 29 46 45 26 42 35 19 17 36  8 21 49 42  3
25 22 15 13 48  6 13 19 25 26 35 24 50 47  1 37  5  7 36  8
42 48  7  6 21  1 49  7 41 20  5 26 21 15  7 50 38 33  9 22
 6 46 19 23 12 28 36  7 49 45 31 33 49 34 29 49 15 37 45 26
 7 35 15 39 22 34 34  4 31 41 32  7 10  5 12 41 23 46 35 38
 9 40 48 50  8  3 21 39  4 21 31 50 49 36 42  6  3 30 42 32
13  7 23 42  1 26 16 24 42 36 26 20  1  6 10 12 16 13 19  4
27 21 21  4 18 17 43 12 42 45 50 46  8 35 29 34 14 41 22 40
31 22 11  1 35 27 49  9 39 26 46 47 32 45 50 17  7 49 31 30
43 24 16 33 46 14 18 46 24 49 26 46 26 34 31 48 21 28 15 38
37 29 33  8 37  6 42 42  9 38 41 41 46 37  1 16 28 41 48 14
 9 43 46  7 50 24 33 19 47 38 50 16 22 44 30 34 49 40 26 17
45 47 48 46 46 40 43 24 45 35 32 11 22 18 41  5 33 32 34 27
35  8 49  1 28  1 29 44 32 19  5 41 22 11 30 36 13 47 13 11
43  2  4 18  4 43 22 17 27  5 43  7 16 31 32  7 31  3 26 44
19 25 18 32  2  5 39  8  4 42 43 15 41  7 39 35 50 25 25 21
23 11 22 33 41  1  5 18 10 40 40 47 37  8 13 46 21  8 17 29
32  1 34 35 46 34 16  4 29 27 25 20 16  7  6 35  2 38 32  9
16  8 28 39 13  9  8 47  2 22 10  8 32  2 26 37 22  6 38 22
49 35 50  3 27  7 20 14 43 49 48  8 41 26  2 44  1 25 10 20
27 38 36  7 28 47 17 31  3  5 45  5 22 22  3 18 11 46 43 13
35 47 26 19 30  2 49 42 40 24 32 40 45  2  2 12 50 27 24 27
14 31 34 13 35 19 24 33 32 48 28 25 34 17 47 32  3 47 42 34
27 14 10 35 49 32 23 46 50 39  5 13 34 26 22  8 10 26 10  5
26 42 13 21  3 34 12 42 16 49 10 11 31  8 17  8 34 37 31 39
18 50 23 11 14 35 17 24 27 35 30 48 15 31 47  8 27 26 12 19
33 29  7 19  8 40 34 50 19 28  3 43  1 19 13  2 47 28 33 37
39 42 40 45 31  4 48 48 31 45 44 20 38 19 21 27 23 35 11  6
11 41 17 49 17  8 49 37 27 11  4 26 36 16  3 23 24  9 22 27
44 33 25  8  7 20  1 42 10 22 40 45 23  1 26  2 23  2 11  8
24 48  5 42 14 14  5  9 35 14 33 18 18 36 14 18 18 22 13 28
42  4 18 25 41 36 19 23 33 26 50  9 45 24 14 27 42 48 20  7
11 26 16  3 44 22 23 24 23 23 17 19  1 21 11  8 38 49 44 17
32  9  9 11  3 12 35 26 28  5 28  6 20  8 46 31 18 48 38  6
13 40 23 40 37 20 29 31 45 30 19 48 44  4 31 20 33 43  8  9
33  8 30  3 20 46  1 45  8 29 32 16 35 31 19 20 42 18 34 16
12 26  1  2 48 49 37 49 10 18 28 32 45 36 17 17 24 13 34 40
23 47 35 44  6  9 27 10 11 23 10 43 31  6  4  1 47 43 34 33
12 28 15  9 35 43 35  4 16 40 36 35 24 29 49 37 35  9 28  3
14 49 33 15 48 26 11 27 30  4 34 47 41 20 26 24 35 17  3 29
21 27  2 37 47  3 15 13 34  5 23 43  7 30 32 22 32 49 49 30
45 38 23 20 39 11 24  3 46  7 28 26 18 16  1  9 17 22 29 29
38 27  4 50  4 41  8 10 40 11 45  1 10  9 24  4  2 10 44 24
 8 29 24 18 10  4 41 37 12 25  9 49 22 26 15 31 40 10  3 48
34 36  3 37 32  2 19 40 48 29 10 39 19 43 25 37 37  7 34 44
```

35	10	13	8	15	45	27	49	38	41	12	44	1	4	12	6	24	42	7	24
34	4	2	39	46	9	6	33	46	35	17	11	26	45	4	30	20	27	46	39
29	24	5	9	14	16	19	16	22	7	31	24	25	8	22	21	47	15	46	48
4	50	12	38	32	37	18	44	25	43	35	26	14	4	38	31	2	13	43	30
49	50	36	49	3	21	10	2	35	33	46	27	19	36	49	17	22	50	27	3
29	50	29	38	34	1	25	31	19	41	40	32	36	12	41	10	45	45	13	41
45	44	49	40	5	19	31	44	2	17	13	46	50	10	3	27	36	22	50	41
3	19	25	47	33	38	3	43	29	21	49	50	1	49	49	43	46	28	48	38
35	15	26	21	44	9	36	35	37	30	39	12	3	4	32	4	32	47	35	23
8	44	25	14	33	40	16	50	17	14	46	6	7	21	7	46	25	20	30	8
46	10	20	34	35	10	34	6	30	47	23	28	21	35	5	8	42	11	7	46
46	19	44	10	42	39	3	28	28	25	26	14	25	36	45	5	9	21	13	43
43	50	40	11	16	49	24	11	21	33	35	4	37	38	50	37	20	8	32	30
28	23	20	10	10	38	5	42	35	12	19	12	31	43	17	12	11	50	6	26
13	12	35	5	30	41	25	10	42	25	2	38	3	7	30	11	24	18	47	3
1	12	44	30	6	48	4	28	13	24	30	41	39	11	32	50	20	34	7	8
49	9	26	25	6	22	15	49	47	16	38	1	29	22	33	5	2	45	43	28
36	43	49	5	6	15	4	30	27	31	17	35	37	16	38	22	28	37	36	1
31	29	37	21	50	35	6	1	45	37	30	18	13	39	2	36	26	49	3	42
8	16	37	29	25	11	13	29	14	9	29	45	17	25	6	37	15	45	19	2
14	14	34	11	21	12	37	40	35	42	21	3	26	15	18	39	20	28	30	38
33	1	19	34	1	11	30	29	16	22	36	33	10	22	12	43	37	3	22	31
6	46	4	22	16	6	50	31	36	40	42	46	43	49	34	7	1	1	34	48
47	23	42	22	25	30	26	38	15	9	14	44	21	2	20	11	2	41	31	15
7	29	39	19	6	26	27	12	25	30	47	37	29	11	10	23	4	46	13	26
44	48	26	4	29	6	26	6	14	11	28	1	8	45	18	17	9	13	38	17
36	22	22	39	18	21	21	26	17	31	46	8	21	28	44	39	23	26	37	30
4	13	49	27	18	30	46	2	24	10	14	29	20	6	47	25	27	28	26	26
20	23	4	25	15	12	41	2	48	21	35	13	12	14	7	15	38	29	31	8
31	9	24	12	49	35	21	2	41	10	16	43	27	43	41	23	32	34	48	34
23	2	47	7	35	23	37	46	11	12	37	11	33	6	24	49	5	48	12	32
35	19	38	34	22	23	45	21	37	19	15	30	5	5	1	3	41	2	13	21
31	35	48	40	20	20	27	17	38	43	26	1	38	47	9	12	31	14	15	26
14	46	34	9	7	5	50	47	37	36	15	32	18	12	39	46	38	8	19	43
39	38	27	32	2	40	38	12	32	6	17	2	36	18	2	29	15	30	33	7
37	50	44	23	29	28	38	21	6	32	24	31	5	40	50	7	18	16	37	8
27	47	11	33	35	25	35	2	2	33	48	41	26	23	43	15	27	6	49	10
32	29	22	20	4	12	20	25	32	32	42	30	7	4	7	44	11	14	43	15
49	4	13	12	28	8	5	14	47	27	12	33	27	22	14	7	44	40	15	29
12	3	26	30	19	35	43	14	6	2	38	40	6	40	35	6	22	43	1	33
14	42	22	46	29	40	41	11	38	47	38	14	17	11	19	48	30	3	41	44
15	47	4	7	15	10	28	45	11	27	38	7	6	42	49	13	9	37	49	38
20	14	30	49	8	33	23	31	49	43	32	27	8	13	17	19	22	20	25	11
34	28	28	11	25	24	50	18	49	1	7	3	15	41	36	41	21	47	29	47
38	29	17	7	41	34	6	16	46	33	3	4	39	2	7	24	13	5	38	37
50	31	22	40	2	20	25	3	31	6	32	3	32	41	38	4	28	35	22	44
44	35	39	15	44	13	48	48	16	44	48	48	2	43	8	22	34	48	5	21
16	49	3	13	6	30	39	25	4	44	7	22	28	50	37	41	6	46	33	24
2	3	4	3	3	47	49	31	1	41	38	18	29	24	47	12	39	39	41	33
42	15	6	8	35	8	36	50	38	26	11	48	28	18	36	43	20	3	20	17
50	9	11	25	10	49	28	24	34	11	50	13	23	38	39	13	38	10	33	50
26	31	25	38	9	12	46	15	11	49	50	22	48	14	46	42	6	31	32	28
29	17	29	40	48	8	12	25	16	47	47	4	43	14	20	3	27	15	24	36
39	7	40	41	3	40	23	11	36	34	31	27	23	14	13	42	8	45	39	15
23	15	34	46	20	16	15	4	9	29	17	15	39	8	33	44	29	13	45	28
6	41	7	10	34	14	27	21	50	6	4	15	47	33	9	1	7	32	17	27
33	45	43	14	35	3	23	37	10	12	2	12	29	29	10	25	18	3	50	19

```
41  4 33 26 37  8  6 48 46 31 39 47  2  8  9 18  7 34 30 34
21 38 40 20 41 25 31 40 39  4 34 32 40 24  4 38  9  4 48 40
34 21 17 42  5 39 29  2  6 45 11 20 40 33 28 14 16 33 17 12
32 49 20 28  9 40 19 49 23  5 17 17 37 14 24 15 40 43 38 45
25  7 29 18 21 42 24 31 34 42 36  4 22 37  4 14 34 32 19 26
39 36 13 26 15 47 41  6 25 34 10 50  7 26 19  9  4 35 39 44
46 49 46  2 37 11  4  5 38  2  1 27 45 26 28 34 30 42 18 12
17 48 24  5 23 15  6 44 34 18 11 32 43 23 10 29 30 16 29 33
 1 40 32 15 13 26  7 49 16 29 47  2 30  7 33  9 30  9 18 14
31  5 11 49 21 20 12 16 42 21 40 25 25 43 21 25 24 29 20 35
49 11 24 32 47 43 26 30 40 33  7 16  2 30 21 33 49  5 27 13
18 33 23  9  1 29 30 31 29 29 23 26  8 28 18 15 45  6  1 24
39 16 15 17 10 19 42 33 34 12 34 12 27 15  3 38 24  5 44 13
20 46 30 47 44 26 36 37  1 37 26  5 50 10 38 26 40 50 14 15
40 14 36 10 27  3  8  1 15 35 38 22 41 37 26 26 49 24 40 22
19 33  8  8  5  6 44  5 16 25 35 39  1 43 23 23 30 20 41 46
29  4 41  1 13 15 34 17 18 30 17 50 38 12 10  8  3 50 40 40
Stop - Program terminated.
```

```
B>RANDO
2500,3215
 253  259  252  222  244
 272  274  240  224  260
Stop - Program terminated.
```

A4 THE CONDUCTIVITY OF A THIN FILM WITHOUT USING THE BOLTZMANN EQUATION

The standard derivation of the electrical conductivity of a thin film involves solving the Boltzmann equation. In this paper we derive the same result using a mean collision time, kinetic theory approach. We also show clearly that the appropriate relaxation time to use in the Boltzmann equation is the bulk relaxation time.

1. INTRODUCTION

Using the free electron model, the electrical conductivity of a bulk metal is calculated to be [26]

$$\sigma = ne^2\tau/m \qquad (1)$$

where n is the number density of conduction electrons, m the mass of the electron and τ the mean time between collisions. Usually the electrons in the metal are described by a degenerate Fermi-Dirac distribution and the mean collision time, or relaxation time, is that for electrons at the Fermi surface. Although all of the electrons contribute to the current flow, it is only those electrons close to the Fermi surface that can be scattered. The electrons deep within the Fermi sea have no nearby empty states to scatter into.

In a thin film additional scattering takes place at the surfaces of the film and this will reduce the mean collision time and hence reduce the conductivity. Only those electrons within approximately one mean free path of the surface experience this additional scattering. The mean free path is related to the mean collision time by $l = v\tau$, where v is the velocity. Only as the thickness of the film approaches the mean free path will there be an appreciable change in conductivity.

The textbooks discussing conductivity [27-29] in thin films generally start with a simple mean free path

approach given by Thomson [30], which has the unfortunate problem of not asymptoting to the bulk conductivity as the thickness of the film approaches infinity, and then proceed to the sophistication of the Boltzmann equation [31]. In this paper we will, in section II, extend Thomson's work to give the correct asymptotic limit, within the assumption of all electrons having the same mean free path. In section III we give a more realistic kinetic theory approach which allows for the electrons to have a distribution of collision times. The standard approach of the Boltzmann equation is looked at in section IV where we show that it gives an identical result to our kinetic theory calculation of section III. We also point out a possible problem in the interpretation of the relaxation time used in the Boltzmann equation. By using the path integral formalism in section V we demonstrate that the appropriate relaxation time is, in fact the bulk relaxation time.

As the object of this work is to compare four different methods of calculating the same quantity, we have made the following assumptions in all cases:

(i) The effect of collisions is to return the electron distribution to its equilibrium form, that is to say, there are no persistence of velocity effects and no factors of $(1-\cos\Theta)$.

(ii) Collisions with the wall are diffuse and therefore also return the electron distribution to its equilibrium

form.

(iii) The bulk mean collision time is the same for all the electrons.

II. THOMSON'S MEAN FREE PATH APPROACH

Thomson [30] formulated his mean free path approach within the frame work of the Drude model. Every electron is assumed to travel the same distance l_0 between every collision, unless it collides with the wall. In terms of our assumption of a constant mean collision time this implies all electrons have the same speed. As shown in figure 1, an electron having its last collision at a height z has three possibilities: If it moves away in the angular range $0 \leq \Theta \leq \Theta_1$, where $\Theta_1 = \arccos[(d-z)/l_0]$ and d is the thickness of the film, it will collide with the upper surface of the film after travelling a distance $(d-z)/\cos\Theta$; if it moves in the angular range $\Theta_1 \leq \Theta \leq \Theta_2$, where $\Theta_2 = \arccos(-z/l_0)$, the next collision will take place in the material at a distance l_0; finally if the electron moves off at $\Theta_2 \leq \Theta \leq \pi$ it collides with the lower surface after a distance $-z/\cos\Theta$.

The mean distance travelled between collisions, whether with the surfaces or within the material, is found by averaging over all values of z and Θ, to be

$$l_{av} = (d/2)[3/2+\ln(l_0/d)]. \qquad (2)$$

This implies a conductivity of

$$\sigma/\sigma_0 = (d/2l_0)[3/2+\ln(l_0/d)] \qquad (3)$$

where σ_0 is the bulk conductivity. When $\ln(d/l_0)$ exceeds 3/2, equation (2) predicts a negative mean free path and equation (3) a negative conductivity, both clearly meaningless.

The textbooks simply dismiss this model as crude and proceed to the Boltzmann equation. In fact the failure of Thomson's model is due neither to the assumption of a fixed mean free path nor to that of completely diffuse scattering at the walls, the latter even being used in the Boltzmann equation. Under the assumptions made, equation (3) is the correct expression for the conductivity, but only if d is less than l_0. The three angular ranges are defined by $\Theta_1 = \arccos[(d-z)/l_0]$ and $\Theta_2 = \arccos(-z/l_0)$. If d is greater than l_0 there will exist a range of z near the bottom of the film for which $(d-z) > l_0$ and Θ_1 will be undefined, and similarly Θ_2 will be undefined at the top of the film. It is the quirk of the calculation that the averaging process copes with arccosines whose arguments are greater than one.

The model can be saved by dividing z into three ranges. If the film has a thickness between l_0 and $2l_0$, then electrons in the range $0 \le z \le d-l_0$ can only hit the bottom surface or collide in the material, electrons in the range $l_0 \le z \le d$ can only hit the top surface or collide in the bulk and electrons in the middle $d-l_0 < z < l_0$ can hit both surfaces, see figure 2. The averaging over z and Θ gives

$$\sigma/\sigma_0 = 1-l_0/4d \qquad (4)$$

which correctly gives $\sigma = \sigma_0$ as $d \to \infty$. The case for $d \geq 2l_0$, in which electrons in the range $l_0 < z < d-l_0$ are essentially in the bulk can be shown to be identical to the case $l_0 < d < 2l_0$.

III. KINETIC THEORY APPROACH

The problem with Thomson's method is the assumption that the electrons travel an identical distance l_0 between collisions in the bulk material. In reality there is a distribution of distances, given by p(l)dl, the probability that an electron will have its next collision after travelling a distance between l and l+dl. It is more convenient for us to work in terms of the time between collisions and we take as our distribution function

$$p(t)dt = \tau^{-1} \exp[-t/\tau]dt \qquad (5)$$

where τ is the bulk relaxation time which is assumed to be independent of velocity.

In the presence of an electric field E, an electron experiences a force -eE. If the electric field is in the x-direction, the equation of motion is

$$v_x = u_x - (eE/m)t. \qquad (6)$$

Since collisions are assumed to return the velocity distribution to the equilibrium distribution, the average value of u_x will be zero and equation (6) becomes

$$v_x = -(eE/m)t. \tag{7}$$

The conductivity is then given by

$$\sigma = ne^2 t/m. \tag{8}$$

To calculate t, let us consider an electron starting at position z and moving with velocity v at an angle Θ, as in figure 3. As it travels through the material the probability that it has a collision is given by equation (5), but after a time $(d-z)/v\cos\Theta$ it collides with the surface. Those electrons that, in the bulk material, would have had their next collision after a time longer than $(d-z)/v\cos\Theta$ are now accelerated only for time $(d-z)/v\cos\Theta$. For electrons arriving at position z with velocity v at angle Θ the average time since the last collision is

$$t_-(z,v,\Theta) = \tau^{-1} \int_0^{(d-z)/v\cos\Theta} t \exp[-t/\tau]dt$$

$$+ \frac{(d-z)}{v\tau\cos\Theta} \int_{(d-z)/v\cos\Theta}^{\infty} \exp[-t/\tau]dt, \qquad 0 \le \Theta \le \pi/2, \tag{9a}$$

$$t_+(z,v,\Theta) = \tau^{-1} \int_0^{-z/v\cos\Theta} t \exp[-t/\tau]dt$$

$$- \frac{z}{v\tau\cos\Theta} \int_{-z/v\cos\Theta}^{\infty} \exp[-t/\tau]dt, \qquad \pi/2 \le \Theta \le \pi. \tag{9b}$$

In both cases the first integral gives the contribution from collisions in the material and the second

integral that from collisions with the surface. It can be seen that the velocity and angle enter only in the combination $v\cos\theta$ which is v_z the z component of the velocity. Using this and performing the integrals in equations (9) we find

$$t^{+}_{av}(z,v_z) = \tau\{1-\exp[-(d-z)/v_z\tau]\} \qquad v_z > 0 \tag{10a}$$

$$t^{-}_{av}(z,v_z) = \tau(1-\exp[z/v_z\tau]) \qquad v_z < 0\ . \tag{10b}$$

The appropriate value of $\bar{t}$ to use in equation (8) is obtained by averaging equations (10) over all values of z and all values of v. The probability distribution for z is just dz/d and for the velocity it is the equilibrium Fermi-Dirac distribution, $p(v)dv = (f_0/n)d^3v$. (For ease of comparison with the Boltzmann equation the distribution function $f_0(v)$ is normalized to $\int f_0(v)d^3v = n$). The averaging over z is trivial giving

$$\sigma/\sigma_0 = 1-(\tau/nd)\int_{v_z<0} v_z(1-\exp[-d/\tau v_z])f_0(v)d^3v$$

$$-(\tau/nd)\int_{v_z>0} v_z(\exp[d/\tau v_z]-1)f_0(v)d^3v. \tag{11}$$

Using the degenerate Fermi-Dirac function which is one for $v < v_F$ and the integral over v_z yields two exponential

integrals

$$\sigma/\sigma_0 = 1 - \frac{3\tau v_F}{8d}F - \frac{3\tau v_F}{2d}F \int_1^\infty (1/x^3 - 1/x^5)\exp[-xd/\tau v_F]dx, \qquad (12)$$

where τv_F is the mean free path of electrons at the Fermi surface.

As we shall see in the next section this is identical to the result obtained by solving the Boltzmann equation.

IV. THE BOLTZMANN EQUATION

The appropriate form of the Boltzmann equation for a thin film is

$$v_z \frac{\partial f}{\partial z} - \frac{eE}{m}\frac{\partial f}{\partial v_x} = \left(\frac{\partial f}{\partial t}\right)_c \qquad (13)$$

where $(\partial f/\partial t)_c$ is the rate of change of the distribution function due to collisions. In the relaxation time approximation

$$(\partial f/\partial t)_c = -\frac{(f-f_0)}{\tau}. \qquad (14)$$

Solutions are sought of the form $f = f_0 + f_1$, where f_1 is small compared to f_0. The perturbation f_1 is the solution to

$$\frac{\partial f_1}{\partial z} + \frac{f_1}{\tau v_z} = \frac{eE}{mv_z}\frac{\partial f_0}{\partial v_x}. \qquad (15)$$

The boundary conditions applied to this equation are that f_1 should be zero at both surfaces for electrons leaving the

surface. This is simply a statement that collisions with the surface result in the equilibrium distribution. The solutions for f_1 are

$$f_1^+ = \frac{eE\tau}{m} \frac{\partial f_0}{\partial v_x} [1 - \exp(-z/\tau v_z)] \qquad v_z > 0 \qquad (16a)$$

and

$$f_1^- = \frac{eE\tau}{m} \frac{\partial f_0}{\partial v_x} \{1 - \exp[(d-z)/\tau v_z]\} \qquad v_z < 0. \qquad (16b)$$

The conductivity is obtained by integrating $v_x f_1$ over all values of z and v. The derivative of f_0 is a delta function at a Fermi surface and the integral can be evaluated using this, which shows explicitly that the required relaxation time is that of electrons at the Fermi surface. Alternatively we can see that the integral over v_x involves

$$\int_{-\infty}^{\infty} v_x \frac{\partial f_0}{\partial v_x} dv_x$$

which can be integrated by parts to give

$$\int_{-\infty}^{\infty} f_0 dv_x \ .$$

Using this and integrating over z leads to equation (11) establishing the equivalence of the two methods.

One might worry about the value of τ to use in equation (14). What is needed is the time constant with which the perturbed distribution at position z relaxes back to the

equilibrium distribution when the electric field is removed. Since the rate at which the distribution relaxes depends on collision process at other positions, it might seem that the distribution would relax faster nearer the walls. In the next section we look at this question by using the path integral method to obtain the distribution function.

V. THE PATH INTEGRAL FORMULATION

In the path integral method [32] the distribution function at time t is evaluated by integrating along a trajectory in phase space, taking account of the collisions that remove particles from the trajectory. For the bulk material this gives

$$f(\mathbf{r},\mathbf{v},t) = \int_0^\infty \tau^{-1} f_0(\mathbf{r}_0,\mathbf{v}_0,t-t')\exp[-t/\tau]dt' \qquad (17)$$

where $\mathbf{r}_0$ and $\mathbf{v}_0$ are the positions and velocities at the earlier time t-t′. Figure 4 shows the situation where we have a surface at r_s that the electron left at time t_s. The integral over t′ must now be broken up into two parts, for those parts of the trajectory within the material and those beyond the surface. For those electrons that would have originated beyond the surface the distribution function is that appropriate to the position of the surface

$$f(\mathbf{r},\mathbf{v},t) = \tau^{-1} \int_0^{t_s} f_0(\mathbf{r}_0,\mathbf{v}_0,t-t')\exp[-t'/\tau]dt'$$

$$+ \tau^{-1} f_0(\mathbf{r}_s,\mathbf{v}_s,t_s) \int_{t_s}^{\infty} \exp[-t'/\tau]dt'. \qquad (18)$$

The integration with respect to time is straight forward leading to

$$f(\mathbf{r},\mathbf{v},t) = f_0(\mathbf{r},\mathbf{v},t) + \int_0^{t_s} d[f(t')]/dt' \exp[-t'/\tau]dt'. \qquad (19)$$

Since $df_0/dt = -(eE/m)(\partial f_0/\partial v_x)$ and $t_s = -z/v_z$ or $(d-z)/v_z$ equation (19) is equivalent to equation (16). The point to note is that, by integrating along a trajectory in phase space it is evident that the value of τ is indeed the bulk relaxation time.

VI. CONCLUSION.

The standard method of calculating the electrical conductivity of a thin film is to use the Boltzmann equation. This involves solving a differential equation which is simple enough for the geometry of a parallel sided slab, but may not be so easy for more complicated geometries. In section III of this paper we have obtained the same result using a mean collision time, kinetic theory approach which does not require the solution of a differential equation. In section II we have shown how a much more simpler kinetic theory approach can be modified to give the correct asymptotic limit as the thickness goes to infinity. In section V we demonstrated that the appropriate relaxation time used in the Boltzmann equation is the bulk relaxation time.

FIGURE CAPTIONS

Figure 1: The three angular regions for Thomson's mean free path calculations.

Figure 2: The divisions of z necessary in Thomson's model when $l_0 < d < 2l_0$. Electrons below the dotted line can not reach the top surface and electrons above the dashed line can not reach the bottom surface.

Figure 3: An electron starting at position z and moving at an angle $\ominus$ hits the surface after a distance $(d-z)/\cos\ominus$, and a time $(d-z)/v\cos\ominus$ if its velocity is v.

Figure 4: The trajectory of electrons whose last collision was at the surface and had their next collision at time t-t'.

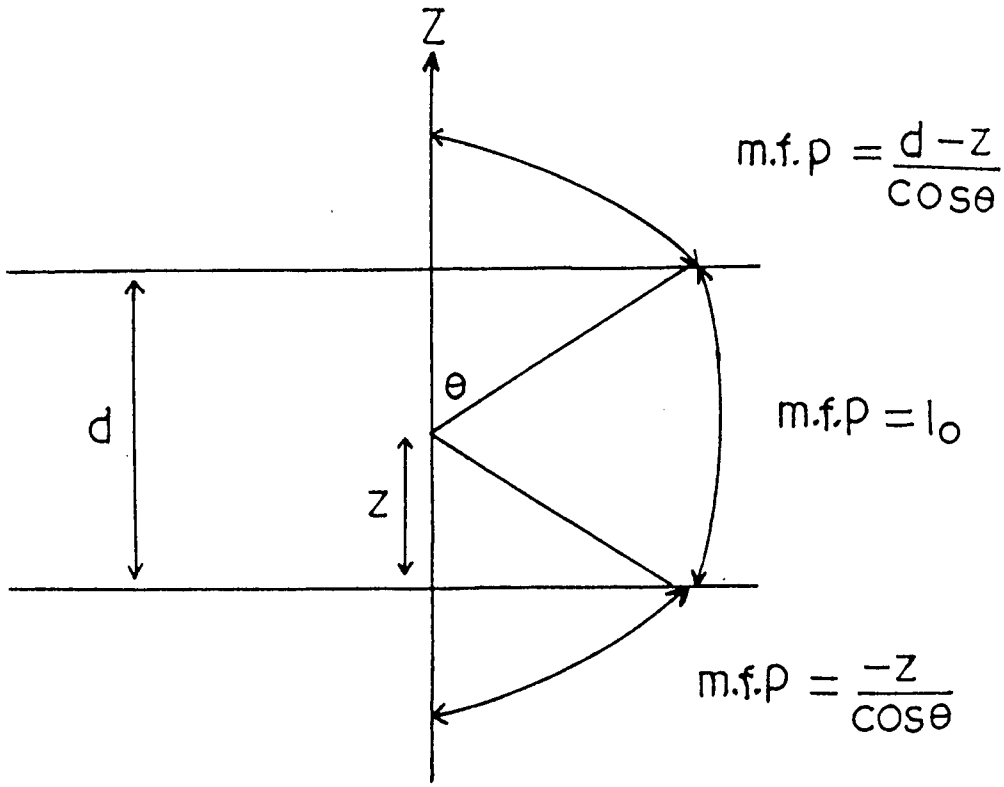

Fig.1

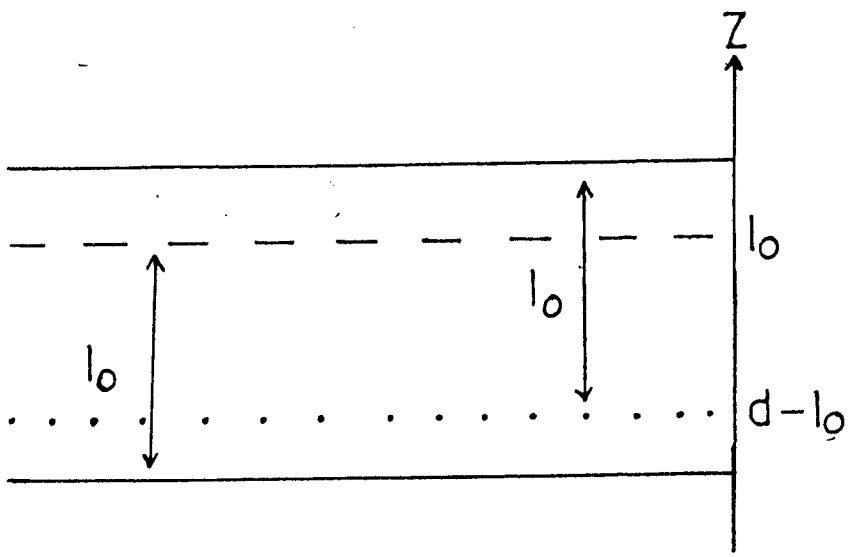

Fig. 2

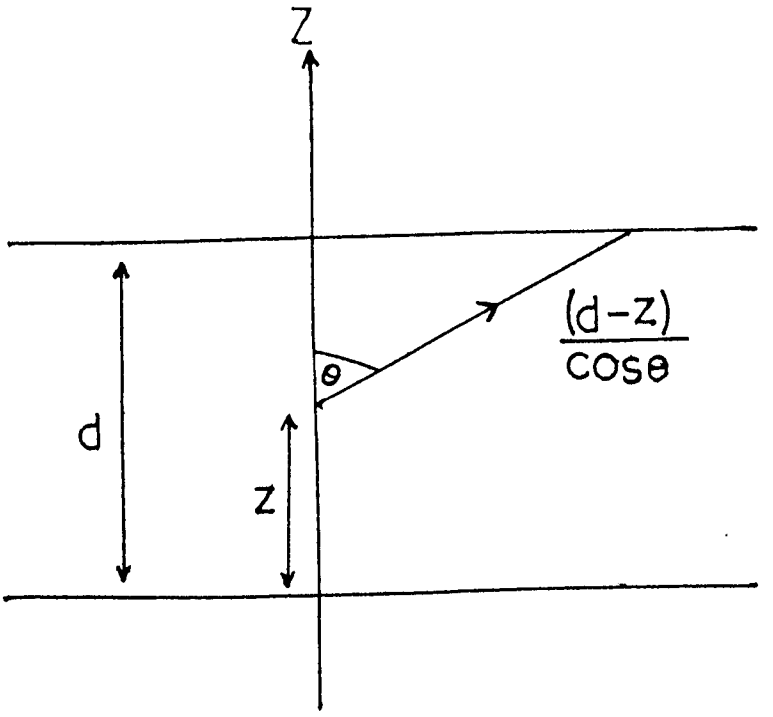

Fig. 3

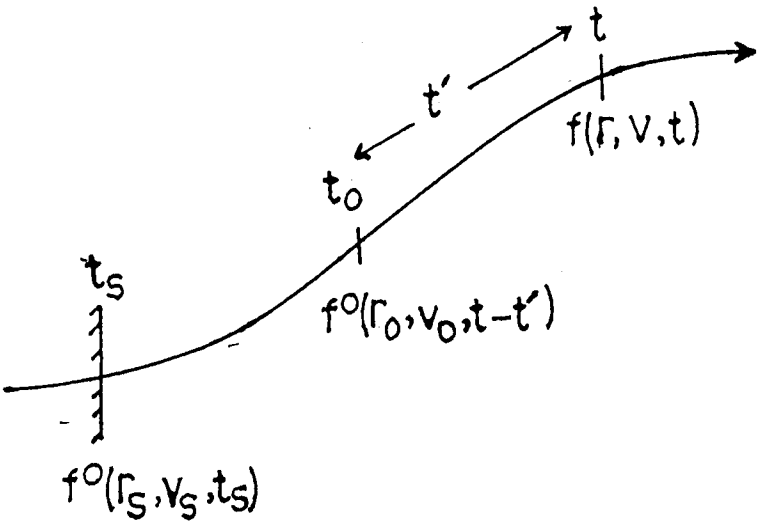

REFERENCES.

[1] R.C. Jones, University of Birmingham, School of Physics and Space Research, "Lecture notes on indroduction to critical phenomena and percolation theory", University of Zambia, Physics Dept., 1992.

[2] C. Kittel, Introduction to solid state physics, (John Wiley & Sons Inc., New York) 6th ed. (1986).

[3] D. Stauffer, Introduction to percolation theory, (Taylor and Francis, London) (1985).

[4] V.K.S, Shante and S. Kirkpatrick, Adv. Phys. **20**, (1971), 325.

[5] D.J. Thouless: Percolation and Localization, course 1, eds., Balian R. et al., (North-Holland, Kingston) (1979).

[6] D. Adler, L.P. Flora and S.D. Senturia, Solid State Commun. **12** (1973) 9.

[7] J.W. Essam: Phase Transitions and Critical Phenomena vol.2, eds. C. Domb and M.S. Green, (Academic press, New York) (1972).

[8] R. Zallen; The Physics of Amorphous Solids, (John Wiley and sons, New York) (1983).

[9] G. Deutscher, Application of percolation, (Elsevier, Tel Aviv) (1987).

[10] E.M. Fisher, Rev. Mod. Phys. Vol. 46 **4** (1974) 597.

[11] K.G. Wilson, Phys. Rev. Lett. **28** (1972) 584.

[12] S. Alexander and R. Orbach, J. Physics. (Paris) Lett. **43**, L625 (1982).

[13] S. Kirkpatrick, Rev. Mod. Phys. **45** (1973) 574.

[14] E.T. Gawlinski and H.E. Stanley, J. Phys. **A14** (1981) L291.

[15] J.M. Ziman, Phys. C: Proc. Phys. Soc., London **1** (1968) 1532.

[16] T.P. Eggarter and M.H. Cohen, Phys. Rev. Lett. **25** (1970) 807.

[17] B.J. Last and D.J. Thouless, Phys. Rev. Lett. **27** (1971) 1719.

[18] B.P. Watson and P.L. leath, Phys. Rev. **B9** (1974) 4893.

[19] R. Fogelholm, J. Phys. C: Sol. St. Phys., **13** (1980) L571.

[20] L.N. Smith and C.J. Lobb, Phys. Rev. **B20** (1979) 3653.

[21] K.H. Han, Z.S. Lim and Lee Sung-ik, Physica **B167** (1990) 185-188.

[22] C.J. Lobb and D.J. Frank, Phys. Rev. **B30** (1984) 4090.

[23] J.G. Zabolitzky, Phys. Rev. **B30** (1984) 4077.

[24] G.E. Pike and C.H. Seager,
Phys. Rev. **B10** (1974) 1421.

[25] H.W. Press, B.P. Frannery, S.A. Teukolsky and W.T. Vetterling, Numerical Recipes (Fortran Version) (Cambridge University Press, New York) (c)1989.

[26] E.G. Ashcroft Mermin, Solid state physics, (Holt-Saunders, New York) (1976).

[27] O.S. Heavens, Thin Film Physics, (Methuen, London) (1970).

[28] K.L. Chopra, Thin film phenomena, (McGraw-Hill, New York) (1969).

[29] D.C. Campbell, The use of thin film in physical investigations, ed. J.C. Anderson, (Academic press, London) (1966).

[30] J.J. Thomson, proc. phil. soc., **11** (1901).

[31] K. Fuchs, proc. camp. phil. soc., **34** (1938).

[32] F. Reif, Fundamentals of statistical and Thermal physics, (McGraw-Hill Kogakusha, Tokyo) 16th ed. (1983)